The Pennsylvania State University

The Graduate School

A SMALL SEMI-AUTONOMOUS ROTARY-WING UNMANNED AIR VEHICLE

A Thesis in

Aerospace Engineering

by

Scott D. Hanford

© 2005 Scott D. Hanford

Submitted in Partial Fulfillment
of the Requirements
for the Degree of

Master of Science

December 2005

I grant The Pennsylvania State University the non-exclusive right to use this work for the University's own purposes and to make single copies of the work available to the public on a not-for-profit basis if copies are not otherwise available.

Scott D. Hanford

The thesis of Scott D. Hanford was reviewed and approved* by the following:

Lyle N. Long
Professor of Aerospace Engineering
Thesis Advisor

Joseph F. Horn
Assistant Professor of Aerospace Engineering

George A. Lesieutre
Professor of Aerospace Engineering
Head of the Department of Aerospace Engineering

*Signatures are on file in the Graduate School.

Abstract

Small, semi-autonomous rotary-wing UAVs have many potential military and civilian applications. A quadrotor, one such UAV with four fixed pitch rotors, has become popular in recent years. This UAV can be highly maneuverable, has the potential to hover and to take off, fly, and land in small areas, and can have simple control mechanisms. However, a quadrotor is unstable and can be difficult to fly. Although electronic stability augmentation can result in stable flight, implementing this in a small quadrotor is a challenging problem because of the small payload capability of these small UAVs. Small, lightweight, and low cost sensors and microcontrollers can be used to control a quadrotor and make the vehicle easier to fly while adding minimal weight, but have limitations such as sensor performance and computing power when compared to larger and more expensive computers and sensors that are used in most flight control applications. The overall goal of this project is to implement these lightweight and low cost sensors and microcontrollers so that they will be useful in the development of a small, semi-autonomous or autonomous quadrotor UAV.

A microcontroller has been interfaced with MEMS gyroscopes, a radio-control (R/C) transmitter and receiver, and motor drivers. A single angular degree of freedom test system with two rotors has been developed to test these electronics. Pilot input from the R/C transmitter and receiver was converted into the desired angular velocity of the system and a desired thrust. The angular velocity of the system is measured with a gyroscope and pilot-in-the-loop PI (proportional and integral) control has been implemented using the microcontroller to calculate the speed of each of the two rotors to maintain the desired angular velocity. The PI control resulted in a decrease in the difference between the angular velocity of the test system and the desired angular velocity. In addition, the amount of pilot input

needed to maintain the desired angular rate of the system was decreased using PI control.

A quadrotor has been developed using commercially available, inexpensive parts for the UAV's frame, brushed motors, electric speed controls, and propellers. The electronics and control system developed for the single degree of freedom test system were extended in this design. Three gyroscopes were used to measure the roll, pitch and yaw rates of the quadrotor. Four pilot inputs, the desired thrust and the desired roll, pitch, and yaw rates, were sent to the quadrotor's microcontroller using the R/C transmitter and receiver. An inexperienced R/C pilot was able to successfully fly the quadrotor for short periods of time. The quadrotor has shown promising characteristics and has the potential to be useful in several future research projects.

Table of Contents

List of Figures viii

List of Tables xi

Acknowledgments xii

Chapter 1
Introduction 1
1.1 UAV history . . . 2
1.1.1 The Beginning . . . 3
1.1.2 Aerial Torpedos . . . 4
1.1.3 Target Drones and World War II UAVs . . . 5
1.1.4 Cold War . . . 7
1.1.5 Vietnam (1964–1975) . . . 9
1.1.6 Israeli UAVs . . . 11
1.1.7 Recent UAV Military Missions . . . 12
1.2 Present-day UAVs . . . 12
1.2.1 Fixed-wing High Altitude Long Endurance Aircraft . . . 14
1.2.2 Small Fixed-wing UAVs . . . 17
1.2.3 Rotary-wing UAVs . . . 22

Chapter 2
Quadrotor Background and System Design 27
2.1 Quadrotor Description . . . 27
2.2 Early quadrotor designs . . . 29
2.3 Recent Quadrotor Research . . . 31
2.3.1 Draganflyer . . . 31

2.3.2 Quattrocopter . . . 32
2.3.3 X-4 Flyer . . . 33
2.3.4 University of Pennsylvania . . . 35
2.3.5 Cornell University . . . 37
2.3.6 Swiss Federal Institute of Technology . . . 39
2.3.7 University of Technology in Compiègne, France . . . 40
2.3.8 Stanford University . . . 41
2.4 System Approach . . . 42

Chapter 3
Quadrotor Hardware **45**
3.1 Microcontroller . . . 45
3.2 Development kit . . . 49
3.3 Gyroscope . . . 50
3.4 Accelerometer . . . 52
3.5 R/C transmitter and receiver . . . 52
3.6 Serial Servo Controller . . . 54
3.7 Electric speed controller . . . 56
3.8 Quadrotor Powerplant . . . 58
3.9 Test Setup . . . 60
3.10 Flight Data Recorder . . . 61
3.11 Hardware Integration and Circuit Design . . . 62
3.12 Quadrotor frame . . . 66

Chapter 4
System Integration and Software **70**
4.1 CCS C compiler . . . 70
4.2 System Integration . . . 71
4.2.1 Gyroscope and A/D Converter . . . 71
4.2.2 R/C receiver and CCP channels . . . 72
4.2.3 Serial Servo Controller and serial communication . . . 74
4.3 Program structure . . . 75
4.4 Control loop . . . 77
4.4.1 Determining angular rates . . . 77
4.4.2 Determining pilot inputs . . . 79
4.4.3 PI control law . . . 80
4.4.4 Driving the motors . . . 82

Chapter 5
Results **84**
5.1 Test System 84
5.2 PI Control Law 87
5.3 Quadrotor flights 90
5.3.1 Pitch rate and input during a flight 92
5.3.2 Angular rates during a flight 92
5.3.3 Euler angles during a flight 96

Chapter 6
Conclusions **100**

Bibliography **106**

List of Figures

1.1 A demonstration of automatically stabilized flight in 1914 3
1.2 The Curtiss-Sperry Aerial Torpedo 4
1.3 A line of Kettering Bugs 4
1.4 The Queen Bee target drone from Great Britain 6
1.5 Reginald Denny and one of Radioplane's target drones 6
1.6 The Pioneer UAV in flight 11
1.7 A graph of weight versus wingspan for several UAVs 13
1.8 The Predator in flight 15
1.9 The weaponized Predator 16
1.10 A picture of the Global Hawk in flight 16
1.11 The Dragon Eye 17
1.12 The FPASS system 18
1.13 The Pointer UAV 18
1.14 The Raven UAV 19
1.15 The Aerosonde UAV 20
1.16 The Aerovironment Wasp 21
1.17 The Aerovironment Hornet 21
1.18 A picture of an R/C helicopter performing an agricultural mission . 22
1.19 The rotary-wing Fire Scout UAV 23
1.20 The MAV from Honeywell 24

2.1 A drawing of a quadrotor showing direction of motor rotation . . . 29
2.2 The Bréguet-Richet helicopter 30
2.3 The Draganflyer quadrotor 31
2.4 The EADS Quattrocopter 32
2.5 The X-4Flyer 35
2.6 A picture of a modified Draganflyer 40

3.1 The PIC development board 49
3.2 A picture of the gyroscope evaluation board 51
3.3 A picture of the accelerometer evaluation board 53
3.4 An R/C transmitter 54
3.5 An R/C receiver 55
3.6 The Mini SSC^{TM} board 56
3.7 A diagram of connections to the ESC 57
3.8 The test system 60
3.9 Schematic of the components connected using the fabricated circuit board 63
3.10 Design of the circuit board 64
3.11 The main circuit board with the two small circuit boards attached at 90 degree angles 65
3.12 Construction of the quadrotor frame 67
3.13 A picture showing the method used to mount the motors to the quadrotor frame 67
3.14 The completed quadrotor 68

4.1 A flowchart describing the interrupt service routine used to sample the gyroscope 73
4.2 A flowchart describing the interrupt service routine used to measure the length of one input pulse from the R/C receiver 75
4.3 A flowchart showing the entire program structure 76
4.4 A flowchart describing the steps used in the control loop 78
4.5 A block diagram describing a system with a PI controller 81

5.1 A graph of the pitch rate of the test system during tests both with and without control feedback 85
5.2 A graph of the pilot inputs for pitch rate of the test system during tests both with and without control feedback 86
5.3 Results of control law for rotation about the pitch axis 88
5.4 Results of control law for rotation about the roll axis 89
5.5 Results of control law for rotation about the yaw axis 90
5.6 The quadrotor in flight 91
5.7 Another picture of the quadrotor in flight 91
5.8 The pitch rate and pilot input for pitch rate during a quadrotor flight 93
5.9 A graph showing the pitch rate of the quadrotor during a flight . . 94
5.10 A graph showing the roll rate of the quadrotor during a flight . . . 95
5.11 A graph showing the yaw rate of the quadrotor during a flight . . . 96
5.12 A graph of the roll angle (ϕ) of the quadrotor during a flight 97

5.13 A graph of the pitch angle (θ) of the quadrotor during a flight . . . 98
5.14 A graph of the yaw angle (ψ) of the quadrotor during a flight . . . 99

List of Tables

3.1 Table of costs for the quadrotor 69

Acknowledgments

I would like to thank my wife, Mandy, and my family for their love and support.

I would also like to thank Dr. Long, my advisor, and Dr. Horn for allowing me to work with them and for all their help and guidance during this project.

I would like to acknowledge the National Defense Science and Engineering Graduate Fellowship and the National Science Foundation Graduate Research Fellowship programs and the Penn State Rotorcraft Center of Excellence for their financial support.

Chapter 1

Introduction

The *Department of Defense Dictionary* defines an unmanned air vehicle (UAV) as "A powered, aerial vehicle that does not carry a human operator, uses aerodynamic forces to provide vehicle lift, can fly autonomously or be piloted remotely, can be expendable or recoverable, and can carry a lethal or non-lethal payload [1]."

There are many potential missions for which UAVs can be useful. Missions which are dull, dirty, or dangerous are considered ideal for UAVs. Long endurance flights, such as the 30 hour missions that were flown from the United States to Kosovo in 1999, can qualify as dull. Pilots flying these missions must deal with issues such as sustained alertness and fatigue that could be avoided through the use of UAVs [1]. A historical example of UAVs performing dirty missions is the collection of radioactive samples after nuclear test explosions in 1946–1948. After 1948, pilots flying manned aircraft while wearing 60 pound lead suits for protection were used to perform this mission. However, these pilot were put at risk when they were trapped by their heavy suits after crashes or from long-term radioactive effects [1]. UAVs can also perform dangerous missions and go in harm's way without

risking a pilot's life. Reconnaisance has been a dangerous mission throughout history, accounting for the highest loss rates for pilots and aircraft during the Vietnam War, and is a good mission for UAVs to perform [1]. In addition to manned reconnaisance missions being dangerous, the failure of these missions can also be damaging politically. When a U-2 was shot down over the U.S.S.R. in 1960 and its pilot was captured, it was an expensive loss not only in terms of money invested in the aircraft and the capture of the pilot, but also politically as treaty negiotiations between the U.S. and the Soviet Union were harmed by the incident [2].

1.1 UAV history

UAVs, or platforms very similar to UAVs, have a long history and have been called many different names, including aerial torpedos, drones, remotely piloted vehicles, unmanned aircraft, unmanned aerial vehicles, and remotely operated aircraft, throughout their history [2]. Several aviation pioneers used unmanned versions of their aircraft to test these vehicles in flight [2, 3]. These models helped in realizing the benefits of wing dihedral and camber. Kites could even be considered the first reconnaisance UAV, as they were used to take pictures during Spanish-American War [4].

Although UAVs were being used before the Wright brothers achieved the first powered, heavier-than-air flight, a lack of technology in the three areas of automatic stabilization, remote control, and autonomous navigation allowed manned aviation to progress more quickly than unmanned flight. Later technology improvements in all three of these areas were critical for the development of successful UAVs.

1.1.1 The Beginning

Nikola Tesla is credited with developing the concept of a remote controlled flying machine. Tesla claimed he was capable of inventing a remote controlled aircraft that " ... could change its direction in flight, explode at will, and ... never make a miss [2]." Tesla demonstrated what he called "teleautomation" in 1898 by making a four foot long boat stop, go, turn left or right, and blink its lights by using different radio signals. Tesla also described his idea for a remote controlled flying machine to Peter Cooper Hewitt, who later would pass the idea on to Elmer Sperry [2].

Elmer Sperry is often credited for establishing the field of unmanned aviation. Sperry was able to use his experience developing gyroscopes to implement automatic stabilization of an aircraft, allowing stabilized flight without any pilot control, and also worked on the problem of remote control. Sperry used three gyroscopes to determine a horizontal reference for any flight attitude. In 1914, Sperry's son, Lawrence Sperry, publicly demonstrated this automatic stabilization in France by flying a seaplane without touching the controls while a mechanic, Emile Cachin, climbed out on the seaplane's wing (figure 1.1) [2].

Figure 1.1. A picture showing Lawrence Sperry's demonstration of automatically stabilized flight in 1914. This picture shows a person walking out on the wing to test the seaplane's automatic stabilization [2].

1.1.2 Aerial Torpedos

The development of automatic stabilization led to interest in using unmanned aircraft as flying bombs or aerial torpedos [2]. Elmer Sperry and Charles Kettering both worked on the development of aerial torpedos: the Curtiss-Sperry Aerial Torpedo (figure 1.2) and the Kettering Bug (figure 1.3). The Curtiss-Sperry Aerial

Figure 1.2. This picture shows the Curtiss-Sperry Aerial Torpedo [2].

Torpedo experienced problems stabilizing itself after launch and a catapult was developed to fix this problem. A distance gear was used to have the aircraft dive towards its target at a prescribed distance. Flight tests demonstrated that this aerial torpedo had an accuracy of 2 miles for a 30 mile flight. The Kettering Bug

Figure 1.3. This picture shows several Kettering Bugs, which were the first production cruise missiles [5].

had several innovative flight controls. The altitude was measured by an aneroid barometer until the aircraft reached its desired altitude, at which point the altitude was maintained with a gyroscope linked to the elevator. Another gyroscope was used to maintain heading and an anemometer was used to determine distance. A subtracting counter was used to determine the distance at which the Bug should dive at its preset target, either by releasing its detachable wings or short-circuiting the ignition [2, 4].

Lawrence Sperry was working on an Army contract to use Messenger biplanes as aerial torpedoes when it was recognized that the unmanned aircraft were navigating as accurately as possible given the current technology. The difficulty in compensating for unpredictable changes in wind conditions was limiting the accuracy of the aircraft navigation. This realization helped result in the first use of a radio to control an aircraft in May of 1922. Heading corrections were sent by radio to the Messenger from an escorting aircraft that flew within sight of the Messenger during tests on targets 30, 60, and 90 miles away. Remote control was also used by the Royal Aircraft Establishment in the United Kingdom to provide inputs to aircraft using a pilot in the loop. Using this radio control, flight speeds of 100 mph and a range of 65 miles were achieved in 1924 [2, 4].

1.1.3 Target Drones and World War II UAVs

The British extended their success in remote control to fly Fairey Queen Bee biplanes, one of which is shown in figure 1.4, as radio-controlled target drones for naval warships [2, 4, 6]. During one of the first demonstrations, the British Fleet fired at a drone for two hours without damaging the Fairey Queen. A contract

Figure 1.4. This picture shows one of the Queen Bees used by Great Britain as target drones [5].

for 420 Queen Bee target drones was signed after the demonstration. This single drone showed the potential invulnerability of unmanned air vehicles when it was used for four months before a warship was finally able to damage the drone.

Reginald Denny, a Briton who moved to Hollywood to pursue his acting career, opened a hobby shop selling model airplanes after his arrival in California and became instrumental in the building of the radio control airplane industry. Denny helped start Radioplane, which built 15,000 target drones for the U.S. military from 1941–1945 for training antiaircraft gunners. Figure 1.5 shows Denny posing with one of Radioplane's target drones. Radioplane, which was bought by Northrop

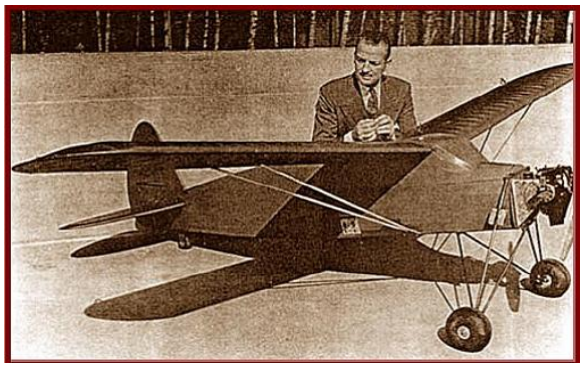

Figure 1.5. Reginald Denny and one of Radioplane's target drones [2].

in 1952, continued to develop unmanned aircraft after World War II, adding film

cameras to their target drones in 1955 to make world's first reconnaisance UAV and producing 48,000 aircraft between 1946 and 1984 [2].

Germans used V-1 cruise missiles, or buzz bombs, to attack England during the last year of World War II (1944–1945). Only 2400 of the 10,500 missiles launched hit their targets. Four thousand of the missiles launched were destroyed by British defenses, illustrating the dangerous nature of these attacks and the benefits of using unmanned systems for these attacks. In addition, 2900 Allied soldiers were killed defending against these V-1 attacks. The success of these buzz bombs encouraged the use of cruise missiles in future conflicts [2].

1.1.4 Cold War

Reconnaissannce missions during World War II resulted in large numbers of lost pilots. One reconnaisance group lost over 25% of its pilots flying missions over North Africa in the first months of fighting there in 1942. By comparison, only 5.5% of American pilots were lost during bombing flights over Germany in daytime from 1943–1945 [2]. Even during fairly peaceful times, reconnaisance can be a deadly mission. Twenty-three aircraft and 179 airmen were lost flying reconnaissance missions from 1946–1990 (not including losses during the Vietnam War). In addition, the Soviet shooting down of a U-2 in 1960 and the trial of its pilot was politically embarrassing and harmed U.S.-Soviet treaty negotiations. The Cold War era marked the beginning of UAV use for surveillance in the U.S. military by the Air Force, Army, and Marines [2].

The Cold War also motivated the need for robotic weapons that were capable of traveling the long distances separating continents while maintaining accuracy high

enough to hit their desired targets. The two competing technologies were intercontinental ballistic missiles (ICBMs) and unmanned aircraft used as intercontinental cruise missiles. Early nuclear bombs were too heavy for ICBMs to carry, but ICBMs had the benefit that their high flight speeds (10,000 mph) allowed them to reach their targets quickly, limiting the accumulation of navigation errors. The unmanned aircraft could carry the weight of the early nuclear bombs because of the aerodynamic lift produced by the aircraft, but their slower flight speeds (500 mph) resulted in long flight times, over which navigational errors were accumulated. Although the ICBM became the dominate technology for transporting nuclear bombs once these bombs became lighter, the attempts to achieve high accuracy navigation systems greatly benefitted the field of unmanned air vehicles [2].

In the attempts to improve the accuracy of navigation systems, inertial navigation systems (INS) became the favored concept because these systems were passive (not required to emit signals) and independent (did not need external inputs). A professor of aeronautics and astronautics at the Massachusetts Institute of Technology, Charles Stark Draper, was the leader in advancing the theory and technology needed to develop, manufacture, and implement inertial navigation systems in several types of vehicles, including aircraft, submarines, and space vehicles. Draper developed the first INS for an aircraft in 1949. Draper's INS allowed a vehicle's navigation to remain accurate even in the presence of turbulence or during aircraft maneuvers without external inputs. INS continued to improve navigational accuracy to such a degree that an INS was able to guide man to and from the moon in the 1960s. Currently, technology such as GPS receivers are often used in UAVs to supplement inertial navigation systems that use ring laser gyroscopes. These

systems can achieve navigational accuracies of less than 20 feet during a 24 hour flight [2].

1.1.5 Vietnam (1964–1975)

The use of UAVs continued in the Vietnam War, during which UAVs proved their abilities, particularly in the large number of wartime reconnaissance missions that the UAVs flew. The Ryan AQM-34 Lightning Bug, or Firefly, was the most used UAV during this conflict. 1016 Lightning Bugs flew 3435 combat missions with a survival rate of 84%. By 1971, two missions were being flown per day and by 1972, UAVs were acheiving 90% success rates [2, 4, 6].

Two missions performed by the Lightning Bug helped illustrate the potential of UAVs. In October 1965, a cooperative mission was performed by the Lightning Bug and two manned aircraft, a U-2 and a RB-47. During the mission, the Lightning Bug intentionally drew fire from surface-to-air missiles while the other two aircraft observed the defense tactics used to attack the Lightning Bug. In the second mission, a Lightning Bug intentionally flew to a known missile site and relayed data on the electronic parameters of the missile's radio-guidance and fusing systems until the bug was hit. The data obtained during these two missions helped make important improvements in U.S. equipment, saving many manned aircraft during the rest of the war.

One challenge that arose during the Vietnam War was the resistance from pilots to the use of UAVs. Pilots did not like their jobs being taken away and the pilots that were flying the UAVs felt like they were being underutilized. A change was made to call the UAVs "remotely piloted vehicles" to help convince crews that

were operating them they were still performing a pilot's function.

As the war continued, the Lightning Bug was used in more ways. Two important developments were the Navy beginning to operate the UAVs from aircraft carriers in 1969–1970 and the use of a real-time video link instead of camera film in 1972 [2].

The demand for the first rotary-wing UAV, the QH-50 DASH, arose when the range of destroyer sonar systems became greater than the range of the destroyer antisubmarine weapons. The DASH, which evolved from a small, one-person helicopter, was designed to extend the range of these antisubmarine weapons by taking off from the deck of a destroyer and attacking hostile submarines using two homing torpedoes carried by the DASH. The date of the first unmanned DASH flight was August 12, 1960 and the DASH was deployed in January of 1963. In addition to antisubmarine warfare, this unmanned helicopter was used in surveillance, gunfire spotting, bombing, cargo transfer, smokescreen laying, and rescue operations. The DASH's capabilities were increased with the additions of a television camera and video data link. Later additions included low light television, a laser rangefinder and target designator, and a moving-target indicator radar. These payloads allowed the DASH to find and fire on targets in all weather and permitted the DASH to be used against troops and convoys at night in an effective manner. Almost 50% of the 810 unmanned helicopters used in Vietnam were lost, but the DASH represented a major milestone for rotary-wing UAVs [2].

1.1.6 Israeli UAVs

Although the U.S. experienced a decrease in interest in UAVs after the Vietnam War, the level of activity with UAVs in Israel was high and eventually helped to recapture U.S. interest in UAVs [2]. During the Yom Kippur War in 1973, Israel used remotely piloted vehicles (RPVs) with radar reflectors to draw fire from ground defenses and then used other RPVs with explosives to determine the location of the radar source and destroy these defenses. This weakened the air defense systems, making them vulnerable to attacks from manned aircraft while decreasing the risk of the pilots performing these manned missions [6]. The use of UAVs in Lebanon in the early 1980s by the Israeli military helped reintroduce U.S. Navy to the capability of UAVs [2]. This led to the use of the Pioneer UAV (figure 1.6), which was produced cooperatively between Israeli and U.S. companies, by the U.S. Navy in 1986 and its continued use today in the Marine Corps [7]. The

Figure 1.6. A picture of the Pioneer UAV in flight [8].

Israeli military and industry have helped Israel become one of the world's leaders in UAV production and innovation and have helped demonstrate tactics such as using unmanned and manned systems together as "force multipliers" [2].

1.1.7 Recent UAV Military Missions

Five models of UAVs were used in the Gulf War (Operation Desert Storm) and although these systems did not play a critical role, they once again showed the possiblities of UAVs in combat [4]. The U.S. Navy successfully used the Pioneer in a "fire spotter role" during this war. Iraqi troops learned that an air attack would follow the appearance of a Pioneer and even surrendered to a Pioneer on one occasion [2].

Surveillance and reconnaisance were provided by UAVs in both Bosnia and Kosovo [2, 4]. The Predator was the primary UAV used in Bosnia. It was flown from a base in Hungary and flew 2700 hours during 332 flights [4]. The Pioneer was used in both Bosnia and Kosovo to provide reconnaisance for Marines in these areas [2].

1.2 Present-day UAVs

UAVs have continually become more prevalent and in the world today there are about 2400 UAVs in operation [2]. Figure 1.7 displays the weight of several of these UAVs versus their wingspans. The use of UAVs can be divided into these areas: 66% of all UAVs are used for commercial activities, 31% for military uses, 2% in non-military or civil applications, and less than 1% for both academic and nonprofit or nongovernment (such as the Red Cross and United Nations) purposes. About 65% of these UAVs are used for agricultural purposes in Japan. Western Europe has the next largest collection of UAVs, which are used for military reconnaisance. The United States has roughly 160 UAVs in operation or evaluation. The military

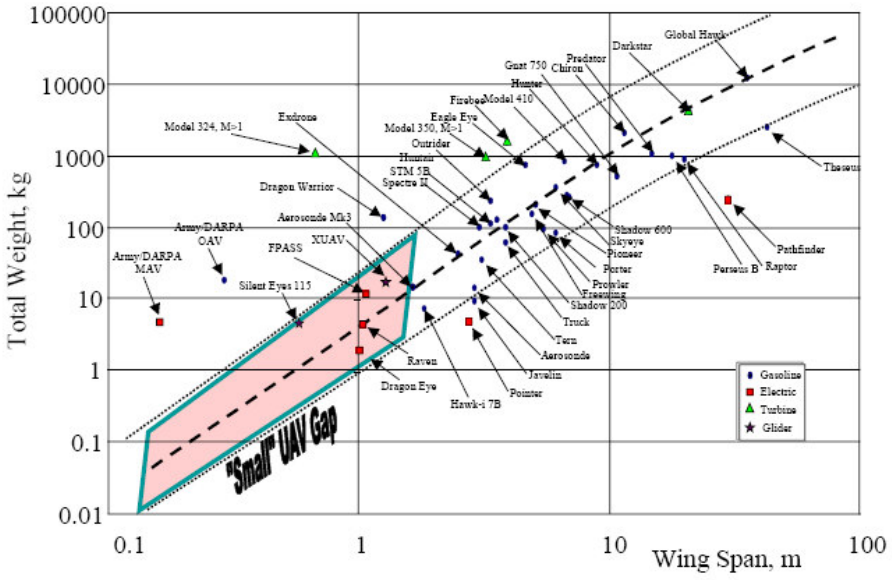

Figure 1.7. This figure shows a graph of weight versus wingspan for many present-day UAVs [8]. This graph shows the relative small number of "small" UAVs compared to UAVs with larger weights and wingspans.

owns most of these UAVs and spent over one billion dollars on UAVs for the first time in 2003. In total, there was two billion dollars spent on UAVs worldwide in 2002. Although the majority of UAV spending and operation occurs in the United States, Western Europe, and Japan, 52 countries around the world either develop, manufacture, operate, or export UAVs. Forty-one of these countries actively fly 80 of the available 250 models of UAVs.

UAVs are generally separated into three classes: high altitude, long endurance aircraft, small aircraft with conventional configurations, and vertical takeoff and landing UAVs [6]. This section describes a few of the current UAVs in each of these classes.

1.2.1 Fixed-wing High Altitude Long Endurance Aircraft

By the 1960s, developments in air defense systems forced reconnaisance aircraft to fly at higher altitudes to ensure they were out of the range of these defense systems. The necessity of flying at these higher altitudes forced aircraft to their limits. The U-2 had to be flown one knot from both stalling and overstressing the airframe. The limitations of orbiting satellites were another difficulty being faced in reconnaisance missions. Orbiting satellites can only provide short glimpses of targets of interest at regular intervals, not the ability to continuously watch these targets. This allowed the subjects of interest to learn when to stop activity to avoid being seen by the orbiting satellites [2].

UAVs are well suited for high altitude (>40,000–50,000 feet) missions and long endurance (>12–24 hours) because of the advantages they offer over manned aircraft performing these missions. Special equipment is needed for pilots to fly at these high altitudes and multiple crew members are needed to fly for these long durations to avoid pilot fatigue [2, 6]. In addition, UAVs can loiter over one area for large amounts of time and can fly over an area at unpredictable intervals.

The area of high altitude long endurance UAVs has seen a high amount of activity since the Department of Defense became interested in this area in the late 1960s [2]. Military and scientific applications have encouraged and benefitted from the high altitude and long endurance capabilities. The potential of solar powered UAVs to fly for weeks or months has raised the possibility of even more UAV missions and resulted in strong efforts to develop solar-powered flight, especially by NASA and AeroVironment [2]. Two well-known high altitude long endurance UAVs currently in use are the Predator and the Global Hawk.

The Predator (figure 1.8) was intended to fulfill military requirements for a UAV that could loiter for 24 hours 500 miles from its base and provide one foot resolution images with a 400–500 pound payload [2]. The Predator has a length

Figure 1.8. The Predator UAV in flight [8].

of 26.7 feet, a wingspan of 48.7 feet, and a gross weight of 2250 pounds [1]. After achieving an endurance of over 40 hours during testing, the Predator was deployed in Bosnia in May of 1995 to provide real-time video surveillance. While in use during the conflict in Kosovo in 1999, the delay in time between the Predator finding a target and a fighter attacking the target allowed many of the vehicles the Predator helped identify as targets to escape. A laser designator and antitank missiles were added to the Predator, allowing a single Predator to find, designate, and attack targets. A Predator equipped with weapons is shown in figure 1.9. This system was tested in 2001 and has been used in Afghanistan and Kuwait to attack terrorists' vehicles [2]. The Predator has a ceiling of 25,000 feet, but the larger Predator B (33 foot length, 66 foot wingspan, and 10,500 pound gross weight) has a ceiling of 50,000 feet [1].

The Air Force's Global Hawk (figure 1.10) from Northrop Grumman has two different model sizes. The lengths of the two model sizes are 44.4 and 47.6 feet, the

Figure 1.9. A picture of the weaponized Predator in flight [8].

wingspans are 116.2 and 130.9 feet, and the gross weights are 26,750 and 32,250 pounds [1]. Five test vehicles had repeatable and reliable performance from 1998–

Figure 1.10. A picture of the Air Force's Global Hawk in flight [5].

2000, reaching an altitude of 66,400 feet and demonstrating an endurance of 31.5 hours. Half of the hours flown by these test vehicles were in civilian airspace, providing valuable experience for flying UAVs with the approval of the FAA and European airspace authorities. The Global Hawk became the first UAV to cross the Pacific Ocean in April 2001, flying from California to Australia. The 7267 mile trip was completed in 23 hours when the UAV landed within feet of the center of the runway in Australia. Global Hawks have been flying combat missions in Iraq and Afghanistan since November 2001 [2].

1.2.2 Small Fixed-wing UAVs

Small unmanned air vehicles (UAVs) can be deployed at the front lines of combat to provide situational awareness to small units of troops through real-time information about surrounding areas [8]. Small fixed-wing unmanned and micro air vehicles (such as the Dragon Eye, Aerosonde, Hornet, and Wasp) have become prevalent and have demonstrated impressive flight abilities and levels of autonomy [1].

The Marine Corps uses the Dragon Eye (manufactured by AeroVironment) at the company/platoon/squad level for reconnaisance, surveillance, and target aquisition missions with a range of 10km. The Dragon Eye (shown in figure 1.11) weighs 4.5 pounds, can carry a one pound payload, has a 3.8 foot wingspan, and is powered with a battery [1].

Figure 1.11. A picture of a soldier holding the Dragon Eye [8].

The FPASS (Force Protection Aerial Surveillance System) from Lockheed Martin (shown in figure 1.12) is used by Air Force security to increase situational awareness through surveillance, the patrol of base perimeters and runway areas, and watching over convoys. The system has six aircraft and a ground station.

Figure 1.12. A picture of the FPASS system [8].

Each aircraft is powered with a battery and has a seven pound weight, a one pound payload, and a 4.3 foot wingspan [1].

The Pointer from AeroVironment is a hand-launched UAV that is battery powered and can be carried in a packpack. The Pointer (figure 1.13) weighs 8.3 pounds, can carry a one pound payload, has a nine foot wingspan, and can be easily assembled from six parts [1, 6]. One hundred Pointers have been bought by the

Figure 1.13. A picture of the Pointer UAV in flight [8].

Marines, Army, and Air Force since 1989 and the United States Special Operations Command has purchased 60 UAVs. Pointers were used in Desert Storm and are currently in use in Iraq and Afghanistan. These UAVs have also been used

by the Drug Enforcement Agency and the National Guard [1]. Pointers have allowed surveillance and reconnaisance missions to be performed quickly and safely. The Pointer's television camera can be used to obtain real-time, high-resolution images while keeping the UAV operator safe [6]. A Global Positioning System (GPS), night vision sensors, and IR imaging technology have also been used on the Pointer and have allowed for night flying and have eliminated the need for visual contact of the Pointer by its operator. These sensors have also helped reduce the interaction the operator must have with the flying Pointer, allowing the operator to perform other tasks while flying the UAV [6].

The Raven (figure 1.14) from AeroVironment is a reengineered Pointer that is smaller than the Pointer (weighs four pounds and has a one pound payload and a 4.3 foot wingspan) thanks to battery and electric motor technology improvements. The Raven requires minimal operator skill and maintenance and was first used in Iraq for "over the hill" and route reconniasance [1].

Figure 1.14. A picture of the Raven UAV in flight [1].

The Aerosonde (shown in figure 1.15) is a small (33 pound weight, 12 pound payload capacity, 9.4 foot wingspan) long endurance (30 hours) UAV [1]. It was the first UAV to complete a transatlantic flight when it flew from Newfoundland,

Figure 1.15. A picture of the Aerosonde UAV in flight [1].

Canada to Scotland in 26 hours and 45 minutes in August 1998 [2]. The Aerosonde is too small to carry a satellite data link so the UAV must be autonomous when it is over the horizon from its ground station, which it was for most of its flight across the Atlantic Ocean. The Aerosonde has flown in many harsh environments, including Alaska. In September of 2005, the Aerosonde was flown into Hurricane Ophelia [9].

The ScanEagle is a small, low cost UAV that is capable of 20 hour flights, weighs 39.6 pounds, can carry a five to seven pound payload, and has a ten foot wingspan [1]. It has a near-vertical recovery system and a pneumatic catapult launcher that allow it to be operated from a variety of take-off or landing locations. These UAVs have been sent to Iraq for force protection of the 1st Marine Expeditionary Force. Its ground station also allows the operator to have the ScanEagle operations integrated with more sophisticated UAVs such as the Predator [1].

The Hornet and Wasp are small fixed-wing micro air vehicles from AeroVironment [1]. The Wasp (figure 1.16) weighs six ounces and has a wingspan of 13 inches. This micro UAV has demonstrated autonomous flight modes such as GPS

Figure 1.16. A picture of Aerovironment's Wasp. Notice the size of the Wasp compared to the pencil in the picture [1].

waypoint navigation, loiter, and altitude and heading hold. It also has forward and side looking cameras. Future goals for the Wasp include adding an optic flow based collision avoidance and navigation system that can be used in areas with poor GPS signals and in urban areas [1]. The Hornet (figure 1.17) has a weight of six ounces and a wingspan of 15 inches. It was the first UAV to be completely powered by

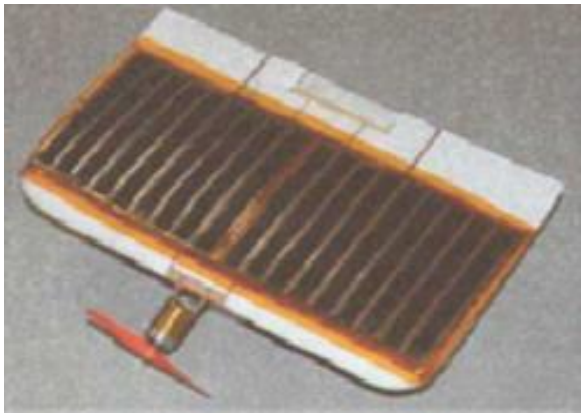

Figure 1.17. A picture of Aerovironment's Hornet [1].

hydrogen. The fuel cell serves as the wing, demonstrating the important idea of using single components to serve multiple functions in very small UAVs.

1.2.3 Rotary-wing UAVs

Rotary-wing UAVs can have capabilities that may allow missions to be performed that can not be considered with fixed-wing UAVs. Even the lightest fixed-wing models must fly fairly fast to provide sufficient lift for flight [10]. These fixed-wing aircraft also need space to turn and although research has demonstrated their capability to fly in small circles over a specified area, they are difficult to fly in confined places, such as urban environments and small indoor spaces [10, 11]. It can be difficult flying fixed-wing UAVs from aircraft carriers and rotary-wing UAVs can allow unmanned flight capabilities from these carriers [6]. Rotary-wing unmanned air vehicles have the potential to be very useful in these situations and this potential has resulted in the development of many of these vehicles.

The most widespread use of rotary-wing UAVs is the use of R/C helicopters (figure 1.18) for agriculture in Japan [2]. There is $100 million worth of commercial

Figure 1.18. A picture of an R/C helicopter performing an agricultural mission [5].

sales of these UAVs annually and companies such as Yamaha have developed industrial unmanned helicopters [12]. There are 6000 licensed operators for the 1565 UAVs that provide one third of the agricultural aviation in Japan. This widespread use of UAVs occured as a result of the decreasing number of rice farmers in Japan. After a government competition to determine a feasible way to deal with this labor shortage, robotic helicopters were selected and their development was

initially subsidized by the government. Each helicopter has been estimated to do the work of 15 laborers and the helicopters cover 10% of the land on which rice is grown in Japan. These R/C helicopters have also been used in civil applications in Japan [2]. After Mount Usu erupted in 2000, manned aircraft were not permitted to fly over the volcano to monitor the advance of ash and mud towards communities at the base of the volcano. To obtain this important information, the Japanese Ministry of Construction used modified versions of the robotic helicopters that had been used in agricultural applications to fly these reconnaisance missions.

Many vertical takeoff and landing (VTOL) UAVs such as the Fire Scout, Hummingbird, and Maverick are currently being developed or used by the U.S. military [1]. The Fire Scout (figure 1.19) from Northrup Grumman has a length of 22.9 feet, a wingspan of 27.5 feet, a weight of 3150 pounds, and a payload capacity of 600 pounds. Over one hundred flight tests have been performed using multiple

Figure 1.19. A picture of the Fire Scout UAV [1].

flight modes including autonomous flight [1, 8]. In addition to these large rotary-wing vehicles, DARPA and the Army are sponsoring a micro air vehicle called the MAV from Honeywell [1]. The goals for the MAV (figure 1.20) are to make a system that can be operated by a single person and can fit in a backpack. The

current ducted fan design weighs 15 pounds, has a payload of two pounds, and has a duct diameter of 13 inches.

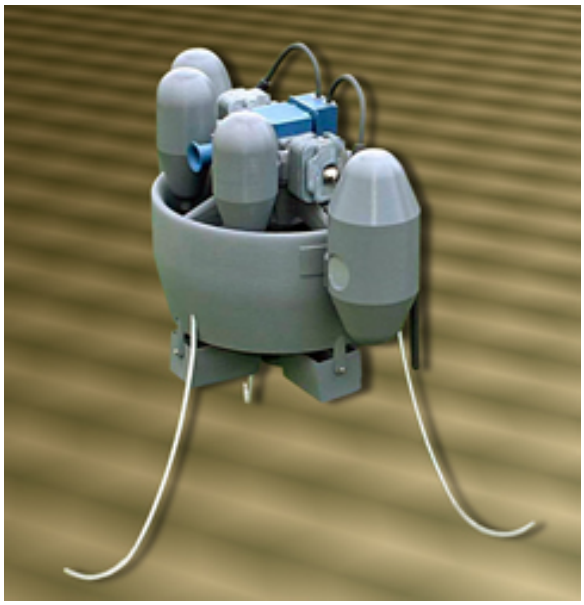

Figure 1.20. A picture of the MAV from Honeywell [13].

University research groups, including those at Georgia Tech, Maryland, Colorado, and Auburn, have also developed rotary-wing UAV systems. Research at the University of Colorado has studied adding low-cost avionics to an R/C helicopter for autonomously calibrating antennae [14]. This group incorporated a custom-made inertial measurement unit with rate gyroscopes and accelerometers and a GPS unit with the goal of achieving autonomous hover using a commercially available R/C helicopter. Researchers at the Georgia Institute of Technology have developed two rotary-wing UAVs: the GTMax, which uses a Yamaha R/C helicopter airframe, has a 10.2 foot diameter rotor and weighs about 157 pounds, and the GTSpy, which uses the MASS Helispy airframe, weighs six pounds and has a 11 inch diameter duct [15]. Using a wide array of sensors, tests have demonstrated many flight capabilities, including fault detection and accomodation, fault-tolerant

flight control, vision-based navigation, vision-based obstacle avoidance, and even launching of the GTSpy from the GTMax during flight. The University of Maryland has also developed two rotary-wing micro UAVs [16]. The MICOR vehicle has two counter-rotating coaxial rotors and weighs 140 grams and the GIANT vehicle has a single rotor and weighs 220 grams. These two vehicles have been flown using an R/C transmitter and receiver and recent research has started to use a five gram inertial measurement unit and optic flow sensors to make these UAVs more autonomous [16, 17]. Auburn University has worked with the Technical University of Delft in Holland on a small ducted fan design that uses adaptive aerostructures [18, 19].

Rotary-wing UAVs, and specifically small rotary-wing UAVs, with VTOL and hover capabilities can have many applications. Small rotary-wing UAVs could be especially useful for indoor flight or for urban missions. Urban combat areas can change very quickly, making it very difficult for soliders to maintain situational awareness. Using UAVs for reconnaisance is also challenging in these situations because of the short line of sight distances and many obstacles. These challenges of the urban combat environment could be met by small autonomous rotary-wing UAVs that are able to fly in areas with many obstacles, poor quality GPS signals, and where communication between the UAVs and their operators are difficult [1].

Incorporating a reliable semi-autonomous or autonomous control system in these small vehicles, so that the operator does not have to constantly monitor their performance or location, will be very challenging since they will only be able to carry the smallest microprocessor systems and power supplies along with very lightweight and inexpensive sensor systems. The software will have to be very

compact to fit in the available memory of the small microprocessors, but powerful enough to provide intelligent control with sensor data of limited quality.

Chapter 2

Quadrotor Background and System Design

A quadrotor is a rotary-wing UAV that has been the subject of several recent research projects. Small quadrotors have many exciting potential missions including flight indoors and in dense urban areas. However, the development of the control systems needed to fly these vehicles can be very challening.

2.1 Quadrotor Description

A quadrotor has four rotors and requires no cyclic or collective pitch. A quadrotor UAV can be highly maneuverable, has the potential to hover and to take off, fly, and land in small areas, and can have simple control mechanisms [20,21]. However, because of its low rate damping, electronic stability augmentation is required for stable flight.

A quadrotor has four motors located at the front, rear, left, and right ends of

a cross frame, as shown in figure 2.1. The quadrotor is controlled by changing the speed of rotation of each motor. The front and rear rotors rotate in a counter-clockwise direction while the left and right rotors rotate in a clockwise direction to balance the torque created by the spinning rotors. The relative speed of the left and right rotors is varied to control the roll rate of the UAV. Increasing the speed of the left motor by the same amount that the speed of the right motor is decreased will keep the total thrust provided by the four rotors approximately the same. In addition, the total torque created by these two rotors will remain constant. Similarly, the pitch rate is controlled by varying the relative speed of the front and rear rotors. The yaw rate is controlled by varying the relative speed of the clockwise (right and left) and counter-clockwise (front and rear) rotors. The collective thrust is controlled by varying the speed of all the rotors simultaneously.

A quadrotor has some advantages over other rotary-wing UAVs. It is mechanically simple and is controlled by only changing the speed of rotation for the four motors [21]. Since the yaw rate is controlled by changing motor speed, a tail rotor is not required to control yaw rate and all thrust can be used to provide lift. A quadrotor may also be able to fly closer to an obstacle than conventional helicopter configurations that have a large single rotor without fear of a rotor strike [10, 21]. The vehicles dynamics are good for agility and its four rotors can allow increased payload [20]. Another advantage of a quadrotor is that minimal cross-coupling simplifies the quadrotor dynamics. However, the dynamics of the quadrotor and specifically its low rate damping can make the vehicle difficult to control [20]. The challenge of controlling the vehicle can be even more difficult for a small, low cost quadrotor [22].

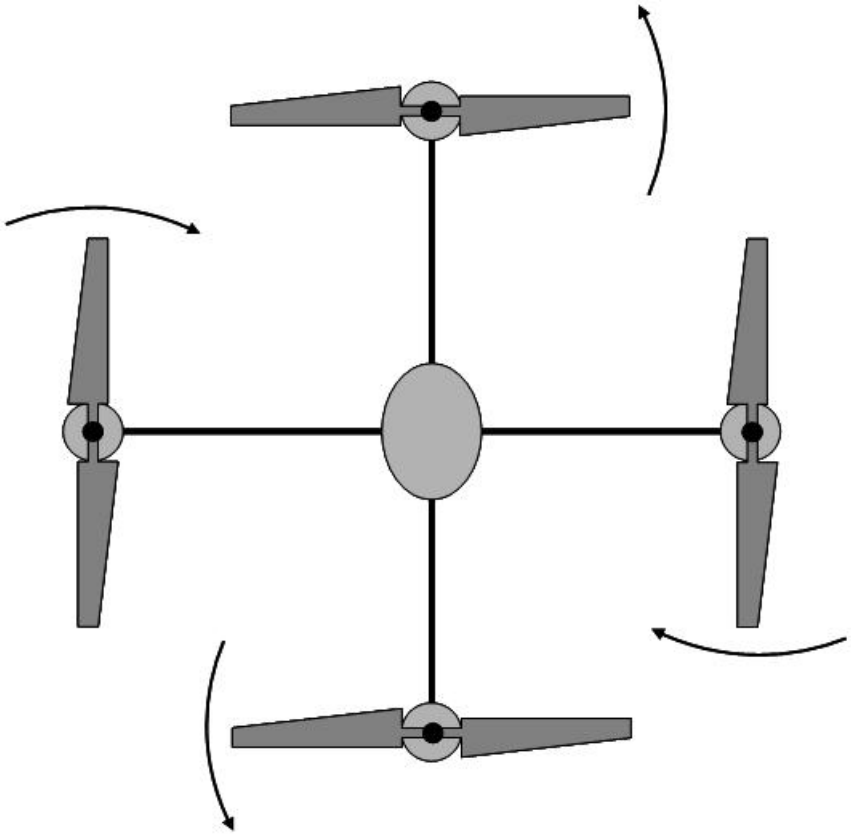

Figure 2.1. A drawing of a quadrotor showing direction of motor rotation.

2.2 Early quadrotor designs

There are a few examples of manned quadrotor helicopters at the beginning of the twentieth century. The Bréguet-Richet Quad-Rotor Helicopter (figure 2.2) was built in 1907 and had a large 8.1 meter rotor placed at each of the four corners of its horizontal cross-shaped frame [23]. Two of the rotors rotated in a clockwise direction while the remaining two rotated in a counter-clockwise direction. The pilot sat in the center of the cross below a single engine that drove the rotors through a belt and pulley transmission. The only control input available to the pilot was the throttle and the helicopter did not have sufficient stability. Photographs taken

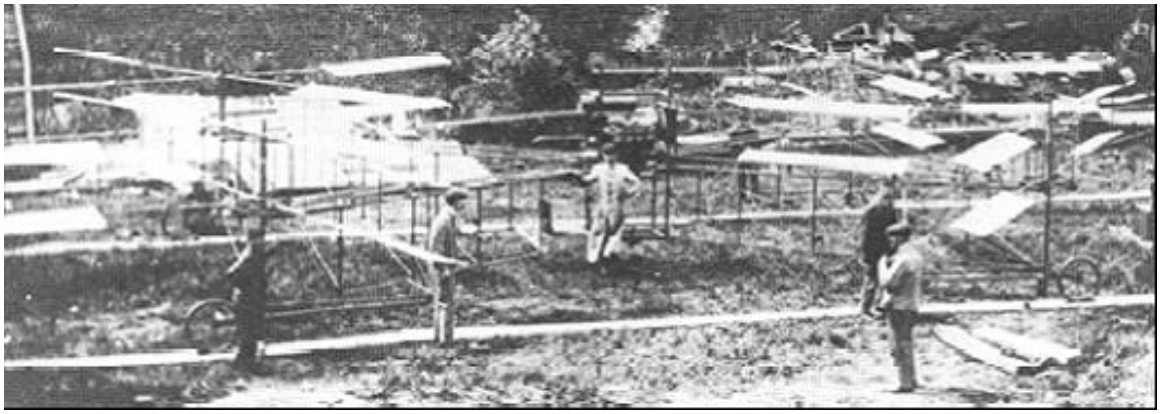

Figure 2.2. A picture of the Bréguet-Richet helicopter [23].

during flight attempts show men at each corner of the frame helping to stabilize and maybe even lift the quadrotor. Although unaided flight was not achieved, the idea of using both clockwise and counter clockwise rotating propellers is a key feature of the quadrotor developed in this research.

Another large quadrotor helicopter was built for the U.S. Army Air Service in Dayton, Ohio in 1921 by George de Bothezat [24]. The helicopter's four rotors were each 26 feet in diameter. All four rotors were turned by a single engine. More than 100 test flights were performed on the de Bothezat helicopter, but the helicopter could not be well controlled in flight, and did not meet U.S. Army performance specifications.

Convertawings built a quadrotor in Amityville, New York in the 1950's. This vehicle had rotors over 19 feet in diameter and wings to create lift in forward flight. Two engines were used in the design and the vehicle was controlled by varying the thrust provided by each rotor. The Convertawings quadrotor was flown successfully, but production was stopped because of a lack of interest in this aircraft [25, 26].

2.3 Recent Quadrotor Research

There have been a large number of papers in recent years describing the dynamics and controls of quadrotor UAVs as well as efforts at constructing and flying these vehicles. Some projects have focused on modeling the dynamics of quadrotors or testing control strategies in simulations [10, 27–30], while the following section describes projects that have attempted to fly quadrotors.

2.3.1 Draganflyer

A well known quadrotor is the Draganflyer (figure 2.3), a commercial product from RC Toys [10, 31]. The Draganflyer is flown using an R/C transmitter and its

Figure 2.3. A picture of the commercially available Draganflyer quadrotor.

onboard electronics. The pilot can control the collective throttle setting for the four motors and the yaw, pitch, and roll rates of the quadrotor. The electronics onboard the Draganflyer include a receiver for pilot inputs, three piezo gyroscopes to sense the angular velocity of the system, a microcontroller to perform control calculations, and motor drivers. The most recent version of the Draganflyer also

includes four infrared heat sensors to allow the quadrotor to level itself while it is being flown outdoors. The Draganflyer has a carbon fiber and high impact nylon frame, has a length of 30 inches from rotor tip to rotor tip, weighs 17 ounces, and can lift a payload of four ounces in addition to its onboard electronics. A rechargeable battery pack is carried onboard.

2.3.2 Quattrocopter

The EADS Quattrocopter (figure 2.4) is a quadrotor unmanned air vehicle that was intended to be a testbed for developing micro air vehicle flight control, but is now being pursued for industrial applications because of its promising performance [32]. The onboard electronics include a micro avionics autopilot that has a six degree

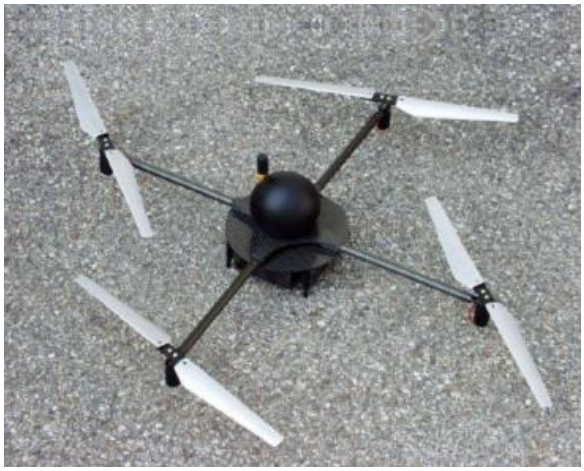

Figure 2.4. A picture of the EADS Quattrocopter [32].

of freedom MEMS inertial measurement unit (IMU), air data sensors, and a GPS receiver, a R/C receiver, a 16 bit analog to digital converter, and power amplifiers to drive the motors. The Quattrocopter is capable of a 20 minute flight with a single charge of its lithium batteries. The vehicle is small (length of 65 cm), weighs about half a kilogram, and has a detachable fuselage so it can be stored in

a backpack. The electric motors allow this UAV to operate quietly. The UAV has a 50% excess power margin to carry out manuevers and to carry small payloads, such as a camera, radar, or acoustic sensors.

2.3.3 X-4 Flyer

Another quadrotor, the X-4 Flyer, is under development in Australia and has been documented in two papers [21, 22]. The electronics used in this project are detailed in the first paper. The use of two inertial measurement units (IMU) were investigated. The first was a commercial IMU from Crossbow that weighed about 475 grams and the second IMU (the Embedded inertial Measurement Unit or EiMU) was developed by a robotics group in Australia [33] and weighed less than 100 grams. The authors stated that the greater weight of the commercial IMU negatively affected the performance of the X-4 Flyer, so the EiMU was used in the final prototype. An onboard computer with two processors is used to record pilot input from an R/C receiver at 45 Hz, a serial interface to the IMU allows data from the IMU to be recorded at 120 Hz (this data is then downsampled to 45 Hz), and a second serial interface is used for asynchronous serial communication to send the pilot input and IMU data to the ground computer at a rate of 45 Hz. This second serial interface is also used to receive control signals from the ground computer and send signals to the speed controllers used to drive the motors.

A non-linear dynamic model of the X-4 Flyer is also presented. This model is linearized about a hover condition and transfer functions relating pilot control inputs to Euler angles (yaw, pitch, and roll) are obtained for this linearized model. These transfer functions were used to develop a pilot augmentation system that

included an inner loop to damp the high frequency dynamics of the system and an outer loop to control the slower dynamics of the X-4 Flyer. Gyroscope signals from the IMU were high-pass filtered to measure angular rates needed for this inner control loop. The outer control loop design was eventually abandoned because of the difficulty in obtaining the attitude of the X-4 Flyer from the IMU and the success the pilot augmentation system achieved using only the inner control loop.

The X-4 Flyer that was built had a weight of 2 kg, a 70 cm frame length, and 11 inch diameter rotors. Flight testing was conducted using a truck battery and tether cord to provide power to the X-4 Flyer. However, these tests were not successful and the thrust margin of the X-4 Flyer was not large enough to allow controllable flight.

The stated goals for improvement after this paper were to design a new X-4 Flyer that would be capable of producing more thrust, weigh less (due to new construction and a lighter IMU), have an onboard power supply that would allow flights of two minutes, and have a wireless serial link and a camera system.

In a more recent paper from the same research group, the X-4 Flyer was re-designed to generate sufficient thrust and manage the unstable dynamics of the X-4 Flyer more successfully [21]. The new design, which is shown in figure 2.5, included inverted rotors and rotor hubs with a teetering design that have springs to provide torsional stiffness. Simulations of the new X-4 Flyer indicate the new design has slow unstable dynamics that may be easily flown by a human pilot or an autopilot. The control electronics are largely the same as the previous version of the X-4 Flyer, but the authors anticipate that the more favorable dynamics of the current X-4 Flyer will allow the control algortihm to be performed with the

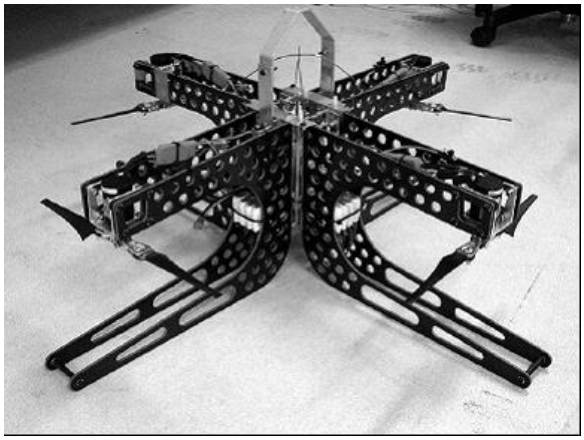

Figure 2.5. A picture of the X-4Flyer [21].

onboard processor, eliminating the need for the ground computer used in the first X-4 Flyer. Flight tests had not been attempted at the time of the paper.

2.3.4 University of Pennsylvania

A research group at the University of Pennsylvania is developing a quadrotor using a commercially available model, the HMX-4, that is similar to the Draganflyer as a testbed [20, 34].

In the first paper, both onboard and offboard computers were used to combine information from inertial sensors and cameras to control the quadrotor [20]. Three onboard gyroscopes are used to stablize the quadrotor in an inner control loop. A camera placed on the ground is used as the primary sensor. Five 2.5 cm colored markers placed on the base of the quadrotor are tracked by the camera and a marker tracking algorithm is used to obtain positions and areas of markers on the image plane. The algorithm then computes the pitch, roll, and yaw angles and the position of the quadrotor. Due to weight limitations of the HMX-4, no GPS or additional accelerometers could be placed on the quadrotor.

The offboard computer receives and processes images from the ground camera, sets goal positions for the quadrotor, and calculates and sends motor inputs to the quadrotor through its parallel port. The onboard computer stabilizes the quadrotor using the gyroscopes and receives motor inputs from the offboard controller through an R/C receiver located onboard.

A model of the quadrotor dynamics was presented and two control strategies, feedback linearization and backstepping, were tested in simulation. The backstepping controller performed better and was implemented experimentally with the quadrotor and a tethering system that prevented excessive translation in the horizontal plane but allowed rotations and vertical translation.

More recently, an onboard camera was added to the quadrotor to develop a two camera method to estimate the position and attitude of the quadrotor [34]. In addition to the five markers on the quadrotor that are seen by the ground camera as in the previous paper, another marker was placed on the ground camera and viewed by the onboard camera. This two camera method had smaller angular and position errors in its estimate of the quadrotor's position and orientation than the other video methods the authors tested in simulations.

Experiments using the two cameras were performed using the HMX-4 and test system described in the first paper [20]. Two separate computers, one onboard and one offboard, were used for vision processing and three gyroscopes were used onboard to stabilize the quadrotor. The new two camera visual feedback system decreased the errors in quadrotor position and orientation from the group's earlier research.

The use of a ground camera to determine the attitude of the quadrotor is useful

for experiments in quadrotor control, but can only be used in unique circumstances on a practical aircraft. For example, the two camera method decribed above could be useful for automated takeoffs and landings at a prescribed location with a stationary ground camera, at a location where a mobile ground robot can be placed, or for other missions that require cooperation between air and ground robots.

2.3.5 Cornell University

Two quadrotor projects have been performed at Cornell University. The goal of the first research project was to develop a method to estimate the attitude of a quadrotor by using an offboard vision system and three onboard gyroscopes [35]. Four LEDs were mounted on the corners of the quadrotor frame and were tracked by three cameras that made up the offboard vision system. The system used an onboard computer, which sent data from the gyroscopes to the offboard computer and sent the motor commands received from the offboard computer to the motors, and an offboard computer, which used the gyroscope and vision data to calculate motor inputs and send the inputs to the computer onboard the quadrotor. A tether was used to provide power to the quadrotor, send the motor commands to the quadrotor, and send the gyroscope data to the ground computer.

A Kalman filter was used to provide a real time estimate of the quadrotor's attitude. The goal of this filter was to provide an estimate that had the low rate qualities of the vision system (10 Hz) and high rate qualities of the gyroscopes (300 Hz). This filter kept the high frequency data from the gyroscopes and the low frequency data from the vision system and attempted to minimize the negative qualities of the gyroscope (sensor drift and bias) and the cameras (low data rate

and latency). The estimate obtained using the Kalman filter showed that the filter was successful in eliminating bias from the gyroscope and the estimate was able to capture high frequency data more quickly than the vision system alone.

The second project at Cornell University was performed as a master's thesis project [36]. This project concentrated on the four thrust producing units and structure of a quadrotor. These two areas were especially important since this quadrotor was heavier (6.2 kg) than the previously mentioned quadrotor designs. The quadrotor frame was designed using Matlab and ANSYS finite element software to determine the appropriate size and strength of the structural components. Despite their expense and the complicated nature of their driving circuitry, brushless motors were chosen for their high power to weight ratios. Propellers with large diameters and low pitch ratios were chosen for their performance in hover (zero forward velocity). The lack of commercially available pusher propellers that rotate clockwise necessitated that custom-made propellers be ordered. The use of lithium polymer batteries with their high energy density and the capability to rapidly drain large amounts of current was another important feature of the design of the thrust producing unit.

This quadrotor had its power supply and sensors onboard. These two components took up half of the vehicle's weight. An inertial measurement unit from Systron-Donner [37] was used. The IMU was subject to drift, but was sufficient for hover tests conducted with a human pilot.

Simulations of the full vehicle non-linear dynamics including force and torque disturbances, sensor bias, and sensor noise were used to design, tune, and test controllers and state estimators. Flight tests were performed with a tether to

prevent damage to the vehicle or its surroundings. There were some successful flights, but a crash occurred and damaged the IMU. Due to the high cost of the IMU, the only option was to repair the damaged IMU, preventing further tests before completion of the thesis.

2.3.6 Swiss Federal Institute of Technology

A team from the Swiss Federal Institute of Technology has worked on the control of angular rates and the height of a quadrotor [38]. Dynamic models of the quadrotor were used to test both classic (PID: proportional, integral and derivative) and optimal (LQ: linear quadratic) control in simulations. Both control algorithms were then used on a quadrotor mounted on a testbed that included a 3D universal joint that contrained height and allowed only angular rotations. An expensive (almost 2000 euros) commercial IMU [39] that uses accelerometers and magnetic references to eliminate sensor drift and a Kalman filter were used to determine the position and orientation of the quadrotor. An offboard PC was used to send orders to the testbed and a PIC microcontroller was used on the testbed for control calculations. The classic PID control was more successful than the optimal control, even allowing an automous flight with cables supplying power from the ground. A possible explanation for the poor performance of the optimal control is because the actuator dynamics were not included in the analysis used to determine the control gain matrix.

2.3.7 University of Technology in Compiègne, France

A research team from France used the commercial Draganflyer quadrotor to study the stabilization of a quadrotor [40]. The gyroscopes that come with the Draganflyer were left onboard and used for an inner control loop intended to stabilize the quadrotor. A 3D electromagnetic tracking system [41] was used to measure position and orientation of the Draganflyer at a rate of 14 Hz. A sensor was placed on the Draganflyer frame that allowed the 3D position and orientation of the Draganflyer to be measured by the Polhemus measuring device on the ground. The device communicated with a computer on the ground using RS-232 protocol. The computer calculated angular and linear velocities numerically from the Polhemus data and then determined control inputs for throttle, pitch, roll, and yaw that were sent to the Draganflyer through an R/C radio. The Draganflyer was able to successfully follow both vertical and horizontal trajectories and is shown hovering in figure 2.6. This research using the Polhemus sensor is useful for practical experiments investigating control of a quadrotor, but to be able to perform useful missions, the quadrotor will need onboard sensors.

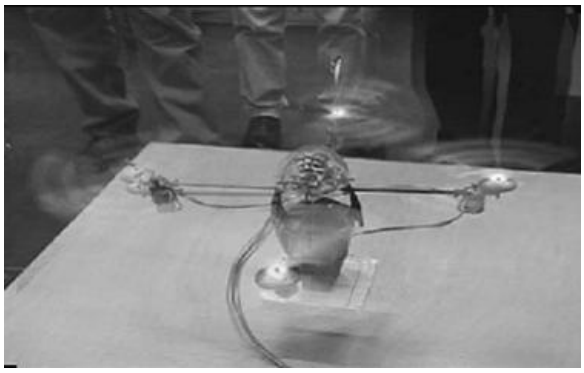

Figure 2.6. A picture of a modified Draganflyer hovering [40].

2.3.8 Stanford University

A modified Draganflyer is being used at Stanford University for the Stanford Testbed of Autonomous Rotorcraft for Multi-Agent Control (STARMAC) [42]. The quadrotor was chosen over conventional helicopters and fixed-wing aircraft as the vehicle for outdoor testing and validation of multi-vehicle control schemes. The electronics that come with the Draganflyer have been replaced with a printed circuit board that was designed and assembled at Stanford. This board performs all of the sensing and communication that is needed for autonomous flight of the quadrotor and has the following components: a commercial IMU called the MicroStrain 3DM-G, two Microchip PIC18F6520 microcontrollers, an ultrasonic sonar sensor, a differential GPS unit (Trimble Lassen LP), and a Class II Bluetooth device that has a range of 150–300 feet and is used to communicate between the quadrotor and the ground station that includes a cluster of personal computers and a laptop with a standard joystick for manual flight.

The IMU uses data from its sensors (angular rate gyros, accelerometers and magnetometers) to estimate the attitude and attitude rate of the quadrotor. The IMU outputs these estimates, which are susceptible to high noise levels and degradation in accuracy when there are large vibrations in the quadrotor frame at high thrust levels. Acceleration data was noisy for all thrust levels and attitude information was used instead of acceleration measurements to estimate translational accelerations. A Kalman filter was used to estimate the vehicle altitude since readings from the ultrasound sensor were unreliable. An infrared distance sensor was added to the system to supplement the sonar measurements during limited parts of the quadrotor flight envelope. Another Kalman filter used GPS measurements,

velocity measurements and attitude information to estimate position and velocity estimates. The GPS data was also used to correct the translational acceleration estimates.

A single quadrotor has performed well in outdoor hover tests during which manual attitude inputs were used in response to wind disturbances while the altitude command remained constant. Once the design for the individual quadrotor is completed, the future goal for this research group is to use new multi-agent control techniques to allow several quadrotors to act as individual agents in a system. The potential for using vision based navigation and control for the individual quadrotors is also mentioned.

2.4 System Approach

Quadrotors will be most useful when they are semi-autonomous or autonomous so that their operator does not have to constantly monitor their performance or location and is able to perform other tasks while flying the vehicle. The short-term goal of this research is to develop a stability augmentation system for a lightweight and low-cost quadrotor that will permit manual flight and to test this system on a quadrotor. This stability augmentation system must be implemented in such a way that the components used in this system will be useful in the development of an autonomous or semi-autonomous quadrotor UAV. The long-term goal of this research is to add additional sensors to increase the autonomy of this inexpensive quadrotor.

Implementing an inexpensive semi-autonomous control system that can be flown on a small quadrotor is a challenging problem because of the small pay-

load capability of these small UAVs. Small, lightweight, and low cost sensors and microcontrollers can help reduce the instability of quadrotors and make it easier to fly while adding minimal weight, but have limitations such as sensor performance and computing power when compared to larger and more expensive computers and sensors that are used in most flight control applications. Since weight is such an important consideration for a small quadrotor, a careful matching of batteries, electric motors, and rotors will be essential. These components will have to be sized to allow the necessary payload to be carried on the quadrotor.

To accomplish the short-term goal of this research, the use of commercially available hardware was emphasized and the design was kept as simple as possible. The microcontroller and MEMS sensors used in this research are both lightweight and low-cost. Microcontrollers do not have a traditional operating system, have no moving parts (such as fans or disk drives), have very low power requirements and are very compact and lightweight. The MEMS sensors are low-cost, lightweight, and commercially available. They can be purchased for as low as 15–30 dollars. Although the sensors can be of high quality, the noise, bias, and drift properties are not as good as those of gyroscopes and inertial measurement units typically used for flight controls. Inexpensive brushed motors were used to keep the cost low and were controlled using electronic speed control units. The rotors were off-the-shelf wood propellers from Zinger Propeller.

In addition, commercial IMUs and commercial quadrotor frames were not used in this project. Commercial IMUs are often expensive, heavy, and output sensor data that has been previously filtered by proprietary filters [33]. These units may also be too expensive to replace or repair if they are damaged in a crash.

Using a commercial quadrotor as a testbed for the control electronics can result in limitations on the payload the vehicle could carry and it could be expensive to repurchase the frame if a crash occurred. The payload limitation could be especially important if an increased payload is necessary to increase the quadrotor's level of autonomy in the future.

Chapter 3

Quadrotor Hardware

This chapter discusses the hardware used in the development of the quadrotor. The commercially available hardware components used in this research and how the parts were physically integrated with each other are described. The system used to test the efficacy of using these hardware components for the quadrotor and the steps used to construct the quadrotor frame are also discussed.

3.1 Microcontroller

The PIC 18F8720 (Microchip Technology, Inc.) 8-bit microcontroller was chosen to obtain data from sensors, input from a pilot, perform control calculations, and control the motors on the quadrotor UAV. This microcontroller has a 25 MHz processor (the current compiler runs the processor at 20 MHz), 68 input/output (I/O) pins, 128 Kbytes of Enhanced FLASH program memory, 4 Kbytes of RAM, 1 Kbytes of data EEPROM. A Guassian elimination code was used to test the number of floating point operations per second (FLOPS) that the PIC is capable of performing. When solving a system of 29 equations consisting of 32 bit float-

ing point variables (which used over 90% of the chip's RAM), 24 kFLOPS were achieved. The PIC does not have an operating system, but simply runs the program in its memory when it is turned on. An important characteristic for using the PIC in an unmanned air vehicle is that the microcontroller requires low current (12 mA typical current draw with a maximum of 20 mA) [43]. This PIC microcontroller also has other hardware features, such as an analog to digital converter (ADC), interrupts, timers, and capture/compare/pulse width modulation (CCP) channels, that are very useful for simplify the interfacing of sensors and motors with the microcontroller.

The PIC 18F8720 has 16 channels capable of performing 10 bit analog to digital conversions. These channels are used to convert an analog voltage (between 0 and 5 volts) to an integer (between 0 and 1023) proportional to the amplitude of the analog voltage [44]. The ADCs on this microcontroller perform their conversions using successive approximation [43]. Successive approximation is accomplished with a digital to analog converter (DAC) and a comparator. For a 10 bit ADC, a 10 bit integer is sent to the DAC, which converts this integer to an analog voltage between 0 and 5 volts. This analog voltage from the DAC is then compared to the analog voltage of the signal to be digitized using the comparator. Usually, this process is started by setting the most significant bit of the integer high and this value (512 for a 10 bit integer) is sent to the DAC. The analog voltage output from the DAC is then compared with the signal's analog voltage. If the DAC output voltage is higher than the signal voltage, the most significant bit is left high. If the signal voltage is higher than the DAC output voltage, the most significant bit is reset to low. Then this process is repeated for each of the remaining bits,

from the second most significant bit to the least significant bit. At the end of the conversion, the 10 bit number represents the analog voltage of the input signal [44]. A single analog to digital conversion takes about 20 microseconds on the PIC18F8720 microcontroller.

This microcontroller is capable of generating interrupts, which cause the program execution to be paused while a user-defined interrupt service routine (ISR) is executed. Program execution then resumes where it was paused after the execution of the interrupt service routine has finished. Examples of events that can be set to cause an interrupt are digital input pins undergoing a transition (5 to 0 volts or 0 to 5 volts), a timer overflowing and resetting to zero, or an incoming RS-232 character. The main advantage of interrupts is that they allow the processor to be told when something needs to be done instead of the processor having to ask if something needs to be done [44].

An example of a situation where interrupts can be useful is when a task needs to be performed when a digital input pin undergoes a transition from low (0 volts) to high (5 volts). An interrupt can be set to occur when the transition takes place. The task that needs to be performed when the pin undergoes a transition can be placed in the interrupt service routine. As soon as the pin transition occurs, the interrupt will happen, the program will be paused, and the interrupt service routine will be executed. Without interrupts, the status of the pin would have to be repeatedly checked in the main program to see if there had been a transition to high. Interrupts allow the response to the transition to be fast and do not require that computational time be used to repeatedly check the state of the pin.

There are five built-in timers (called timers 0–4) in the PIC 18F8720 that can

be used with a great deal of flexibility. All of the timers can use the internal microcontroller clock that increments every 0.2 microseconds as an input. The number of increments before the timer resets, or overflows, and starts counting from zero again can be programmed for each timer. The timer input can also be divided by specified integers. This means that if the internal clock is chosen to be the input and is divided by 2, the timer will increment every 0.4 microseconds instead of the normal 0.2 microseconds. The timers can also be set up to generate interrupts when timer overflows occur. Timers 0, 1 and 3 can also use an external pin as their input. When this input is chosen, the timer increments once for every time the pin undergoes a cycle from low to high to low and acts as a counter.

There are five capture/compare/pulse width modulation channels on the PIC. Each channel can be set to perform one of the three functions. The compare function monitors an analog input voltage. When this input voltage is equal to a specific reference voltage, a digital output pin can be set to 0 or 5 volts, an interrupt can occur, or a timer can be reset.

The capture setting is valuable for measuring the length of a digital pulse. An interrupt can be generated on the falling or rising edges of digital pulses or after every 4 or 16 pulses. The value of a timer is copied to a variable unique to each CCP channel when the interrupt occurs.

The pulse width modulation (PWM) mode is used to generate a square wave, a digital pulse whose signal is high for varying lengths of time. PWM signals are often useful for driving motors.

3.2 Development kit

The CCS C compiler and Embedded C Language Development Kit, with its In Circuit Debugger/Programming Unit (ICD-U40) was used to program the PIC 18F8720 microcontroller [45]. The development kit, which cost $120, includes a development circuit board, shown in figure 3.1, that is 2.5 inches by 4.13 inches, weighs 1.6 ounces, and must be powered by a DC voltage source between 7 and 15 volts. The development circuit board from CCS, Inc. can be bought separately for $60. The PIC 18F8720 microcontroller can be bought by itself for $17.

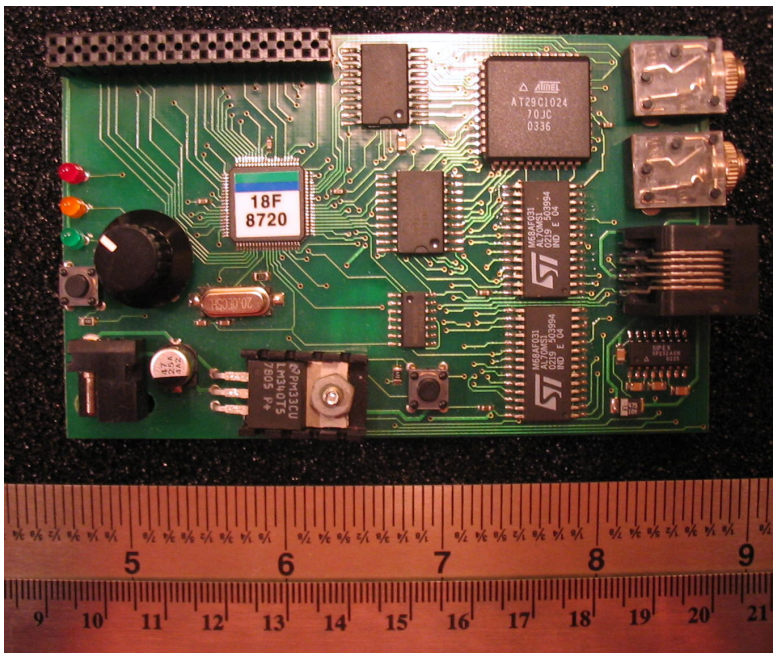

Figure 3.1. A picture of the PIC development board. The PIC microcontroller is the chip labeled 18F8720. The top ruler is in inches and the bottom ruler is in centimeters.

This board contains the PIC microcontroller, a header with two rows for accessing the microcontroller input/output pins, two serial ports, a connector for the In Circuit Debugger (ICD), and other hardware including a voltage regulator and oscillator crystal. There are also three LEDs, a potentiometer, and a push button

to help with programming and debugging. The ICD connects the PIC development board and a PC through a USB connection and allows program variable values to be watched and statements to be printed to the computer monitor, a break point to be inserted into the program, and programs to be stepped through line by line. The two serial ports provide built-in buffering for sending and receiving serial data and MAX232 hardware to convert serial data from the PIC to the RS-232 protocol. These serial ports can also be used to print information to a computer monitor without the use of the ICD.

3.3 Gyroscope

A single chip rate gyro evaluation board (ADXRS150EB from Analog Devices, Inc.) can be used to measure angular velocity [46]. The evaluation board, shown in figure 3.2, weighs three grams, is about 1 inch long by 0.5 inches wide and costs $50. This board is also available in a surface mount chip that measures 7 mm x 7mm x 3mm and costs $30. However, the evaluation board does not require any external resistors or capacitors for the gyroscope to be used. Also, the difficult soldering of the gyroscope's ball grid array that is necessary when using the surface mount chip has already been performed on the evaluation board.

The sensor uses a resonator gyro that senses Coriolis motion and is capable of measuring $+/-150$ degrees per second of angular velocity. The gyroscope includes signal conditioning electronics to help preserve the signal in noisy environments. The bandwidth of the surface mount chip can be set using external resistors and capacitors. The bandwidth of the evaluation board is fixed and set at 40 Hz. The chip produces an analog voltage output (between 0.25 and 4.75 volts for a 5 volt

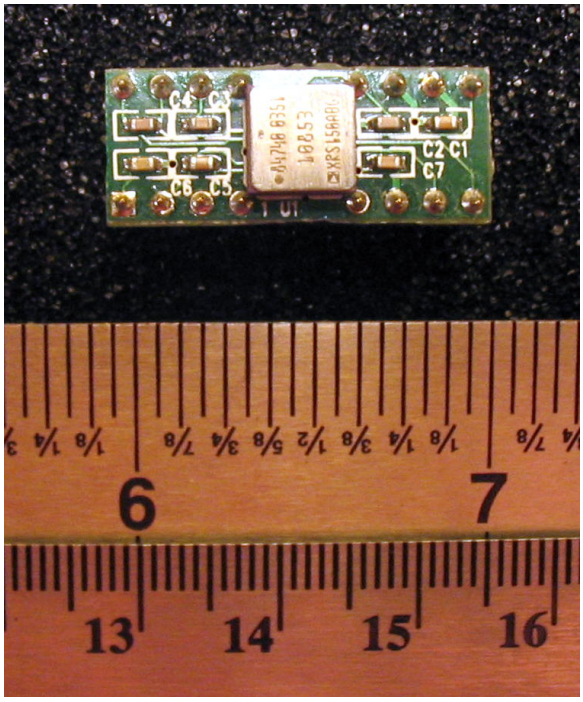

Figure 3.2. A picture of the gyroscope evaluation board with two rulers (inches on the top ruler and centimeters on the bottom ruler).

source) that is proportional to the angular velocity about the axis normal to the top surface of the gyroscope package. The voltage increases for clockwise rotation (while looking down at the top of the chip) of the gyroscope. The noise density of the gyroscope, which is defined as the average noise at any frequency (f, in Hz) in the bandwidth of the part, is 0.05 degrees per second per $\sqrt{\text{f}}$. The initial null point is 2.5 volts, but this can change by a maximum of 300 millivolts for a temperature range of -40 to 85 degrees Celsius. The sensitivity of the gyroscope varies from 11.25 to 13.75 millivolts per degree per second over the gyroscope's operating temperature range.

3.4 Accelerometer

A dual-axis accelerometer from Analog Devices, Inc. (ADXL210EB) was also interfaced with the PIC microcontroller [47]. The evaluation board shown in figure 3.3 is 3/4 inch by 7/8 inch, weighs 5 grams, and costs $30. This accelerometer is capable of sensing accelerations of +/− 10 g's in two perpendicular axes and is also available in a 14 pin dual inline surface mount package that is about 8 mm x 10 mm x 5 mm and costs about $15. The sensor chip produces a digital pulse proportional to its acceleration along two axes by using a duty cycle modulator that is included as part of the sensor chip. The noise density of the accelerometer is 500 micro g's (μg's) per $\sqrt{\text{f}}$, where f is the frequency in Hz. The accelerometer's initial offset at rest (0 g's) can be between −2 and +2 g's and also changes with temperature at a rate of 0.002 g's per degree Celsius between −40 and 85 degrees Celsius. Temperature drift can also change the accelerometer measurements during motion by +/− 0.05% of the accelerometer output.

3.5 R/C transmitter and receiver

An R/C transmitter and receiver were used to send pilot inputs to the quadrotor. These components are often used to control servo motors on R/C (radio-controlled) airplanes, cars, and other vehicles. The signals sent between the transmitter (figure 3.4) and receiver (figure 3.5), are pulses that have a frequency of about 50–60 Hz (which corresponds to a period of 16–20 milliseconds). The high portion of the pulses usually has a range of 1 to 2 milliseconds (ms). A range in pulse length of 1–2 ms will result in a 90 degree range of motion for a servo motor. This range

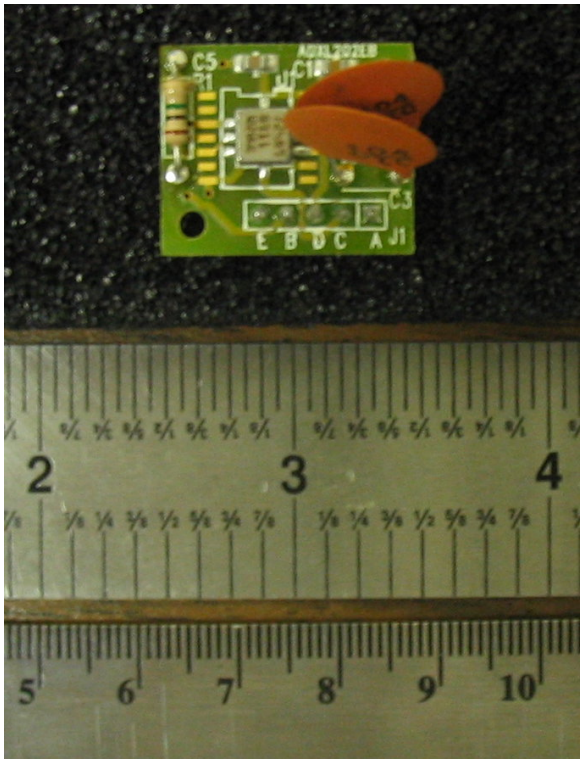

Figure 3.3. A picture of the accelerometer evaluation board with two rulers (inches on the top ruler and centimeters on the bottom ruler).

of motion is often satisfactory for use in many applications because they are often connected to mechanisms that do not need more than 90 degrees of motion [48]. The range of motion of some servos can be increased by sending pulses that are high for less than 1 ms or greater than 2 ms.

The transmitter and receiver are capable of communicating six channels (Futaba model 6EXA) [49]. This model costs about $180, but less expensive models could be used as well. The receiver has three pins for each channel: a positive voltage pin with a voltage equal to the voltage of the power supply used by the receiver (five volts from the PIC development board in the quadrotor setup), a reference ground, and a pin to carry the servo signal.

Figure 3.4. A picture of the R/C transmitter.

3.6 Serial Servo Controller

The Mini SSC^{TM} II, a serial servo controller from Scott Edwards Electronics, Inc. can control multiple servo motors through serial communication [50]. A SSC circuit board (figure 3.6) is 1.4 inches by 2.1 inches, weighs 0.6 oz, and costs $60.

The board contains a PIC microcontroller, eight servo connectors, connectors for supplying power to the microcontroller, and connectors for the data and ground pins used for serial communication. There are three settings that can be configured using jumpers on the circuit board: the baud rate used for serial communication (2400 or 9600), the range of motion for servos (90 or 180 degrees), and the numbers of the motors to be controlled (0–7 or 8–15). SSC boards with different motor numbers can be ordered so that 255 motors can be controlled using a single serial

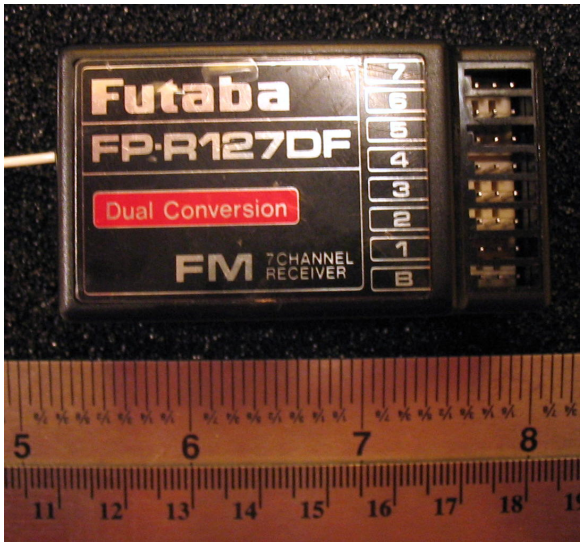

Figure 3.5. A picture of the R/C receiver with two rulers. The top ruler is in inches and the bottom ruler is in centimeters.

input.

The power requirements for the PIC microcontroller on the SSC board are 7–15V and 10 milliamps (mA). The servo motors that are controlled by the board also need to be supplied with power and these requirements vary depending on the motor application.

The SSC board must receive a specific three byte sequence of serial data to control a servo motor. The first byte, called the sync byte, must be set to 255 and tells the SSC that a three byte servo command sequence has started. The second byte indicates the servo motor to which the current three byte sequence is being sent (the motor numbers can range from 0 to 254). The third byte is the desired position of the servo motor, which can also range from 0 to 254. The numbers sent to the SSC board must be sent as individual byte values, not the text representation of these numbers. To monitor serial communication with the SSC board, a green LED on the SSC board can be used. This LED turns on

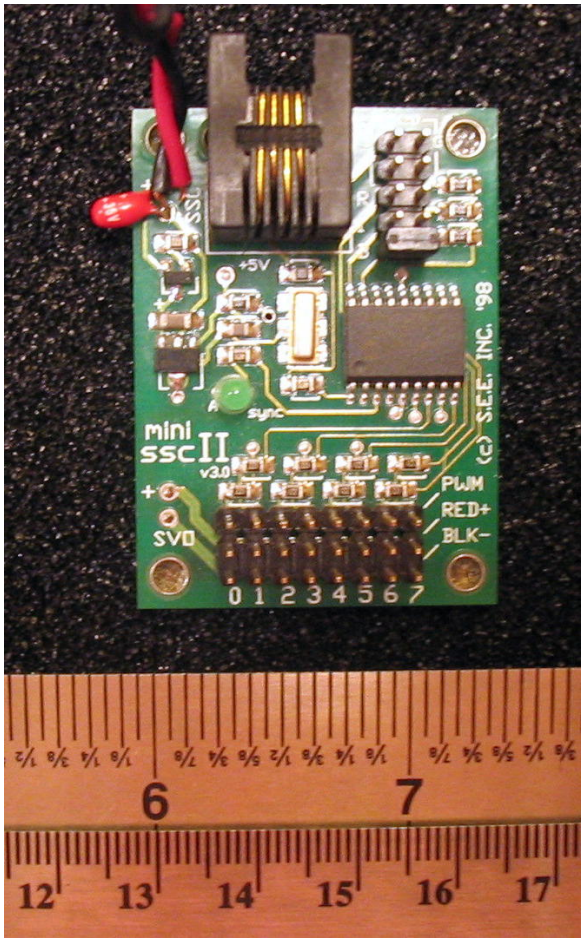

Figure 3.6. A picture of the Mini SSC^{TM} board and two rulers. The top ruler is in inches and the bottom ruler is in centimeters.

after successful initialization of the SSC's microcontroller. After initialization, the LED turns on after the first two bytes are received, and then will turn off after the third byte, the position byte, is received. This LED can provide useful information about the status of the SSC board serial communication [48].

3.7 Electric speed controller

Electric speed controllers (ESCs) are used to convert an input signal (such as from the SSC board or an R/C receiver) with low current into a voltage and current

capable of driving a motor. The 217D from AstroFlight, Inc. was used for the quadrotor [51]. This ESC is rated for a continuous current of 40 Amps, weighs one ounce, and costs about $20. This versatile ESC can be powered by battery packs that have 6–16 nickel cadmium cells or 2–5 lithium polymer cells. These controllers have three sets of connections that are shown in figure 3.7. One is to receive the input signal, one is for a battery to drive the motor, and one is to output the voltage specified by the input signal to the motor. The connection from the input signal is the same as a servo connector and has three pins: a positive voltage, a reference ground, and the signal. The connections with the motor and the battery to drive the motor both have positive and negative terminals.

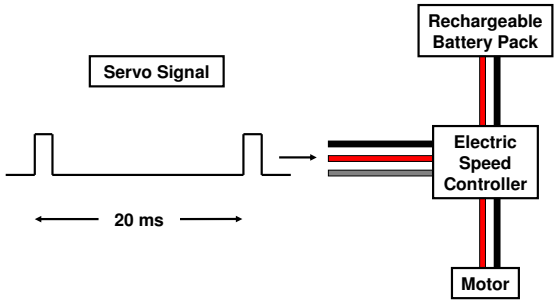

Figure 3.7. A diagram of connections to the ESC.

The voltage supplied to the motor is varied by turning the motor on and off very quickly at a frequency of 2.8 kHz (a frequency faster than the time constant of the motor helps keep the motor speed constant). This is the same technique used by the microcontroller's PWM channels. For example, for the motor to run

at approximately half of its full speed, the motor is turned on and off for equal amounts of time. To increase the speed of the motor, the percentage of time that the motor is on is increased.

There is a safety feature on the speed controller that prevents the controller from activating until it receives a radio signal corresponding to a short pulse (1 ms high) for a duration of one second. When the speed controller is being used on an aircraft with a single motor, this means that the throttle control on the radio transmitter must be held in its lowest position for one second for the controller to be activated and allow the motor to turn on.

3.8 Quadrotor Powerplant

In choosing the components to be used for the quadrotor's powerplant, the software program MotoCalc (version 7.09) from Capable Computing, Inc. was used to determine the combination of components that would meet the desired requirements for flight length, aircraft weight, and thrust production [52]. A flight length of 15 minutes, a time considered adequate to perform a worthwhile mission, was required. A thrust to weight ratio of 1.5–2:1 was deemed high enough to lift the quadrotor and provide sufficient control effort.

A rechargeable battery was selected to provide power to the motors and the SSC board. It was important for the battery to be lightweight, have enough capacity for the desired flight length, and be able to provide high amounts of current that may be drawn by the motors. A rechargeable lithium polymer battery from Thunder Power met all of these requirements and was selected for use on the quadrotor. The battery has 3 cells for a total voltage of 11.1 volts, has a capacity of 2100

milliAmp-hours (mAh), and weighs 5.1 oz. It can provide a continous discharge of 21–25 Amps and a burst discharge of 33 Amps. The battery costs $85.

The motors and gearboxes used for the quadrotor were purchased as a single unit from Grand Wing Servo for about $10. The GW/EPS-100C-DS/BB power system, with a gear ratio of 6.60:1 was chosen. Each power system weighs two ounces. Two pairs of counter-clockwise/clockwise wood propellers with diameters of 14 inches and pitches of six inches from Zinger Propeller were used in the quadrotor. Each pair of propellers cost $15. A propeller with a large diameter and small pitch was found to provide high static thrust, which is very important for the hovering manuevers that the quadrotor will perform. The propellers have 1/4 inch diameter holes and the motor/gearbox systems have three mm diameter shafts so propeller adapters were needed to secure the propellers on the motor/gearbox shafts. A collet propeller adapter, the MPJ-8031 from MP-Jet, that fits a motor shaft of three mm and a propeller hole of five mm was found [53]. Each propeller adapter cost $5. A plastic tube with a 1/4 inch outer diameter provided a perfect fit between the adapter and the propeller.

Simulations performed with Motocalc using this combination of battery, motor/gearbox systems, and propellers predicted that the requirements for length of flight and thrust to weight ratio would be satisfied. At full power, a thrust of 49 ounces was predicted. The total weight of the quadrotor with the parts used in the simulation was estimated to be 32 ounces. Therefore, at full power, the thrust to weight ratio was predicted to be about 1.5:1 and the flight time was estimated to be about 10 minutes. In addition, the current being drawn from the battery was estimated to be 12.5 amps, which is within the specifications of the battery

pack. The flight time at full power is less than the desired length, but when the power supplied to the motors is decreased to generate only the thrust needed to hover (32 ounces), the estimated flight time is increased to about 23 minutes.

3.9 Test Setup

A two-rotor test system, shown in figure 3.8, was developed to test the hardware components described earlier in this chapter by implementing a pilot-in-the-loop control law. A motor/gearbox system and a propeller were mounted to each end

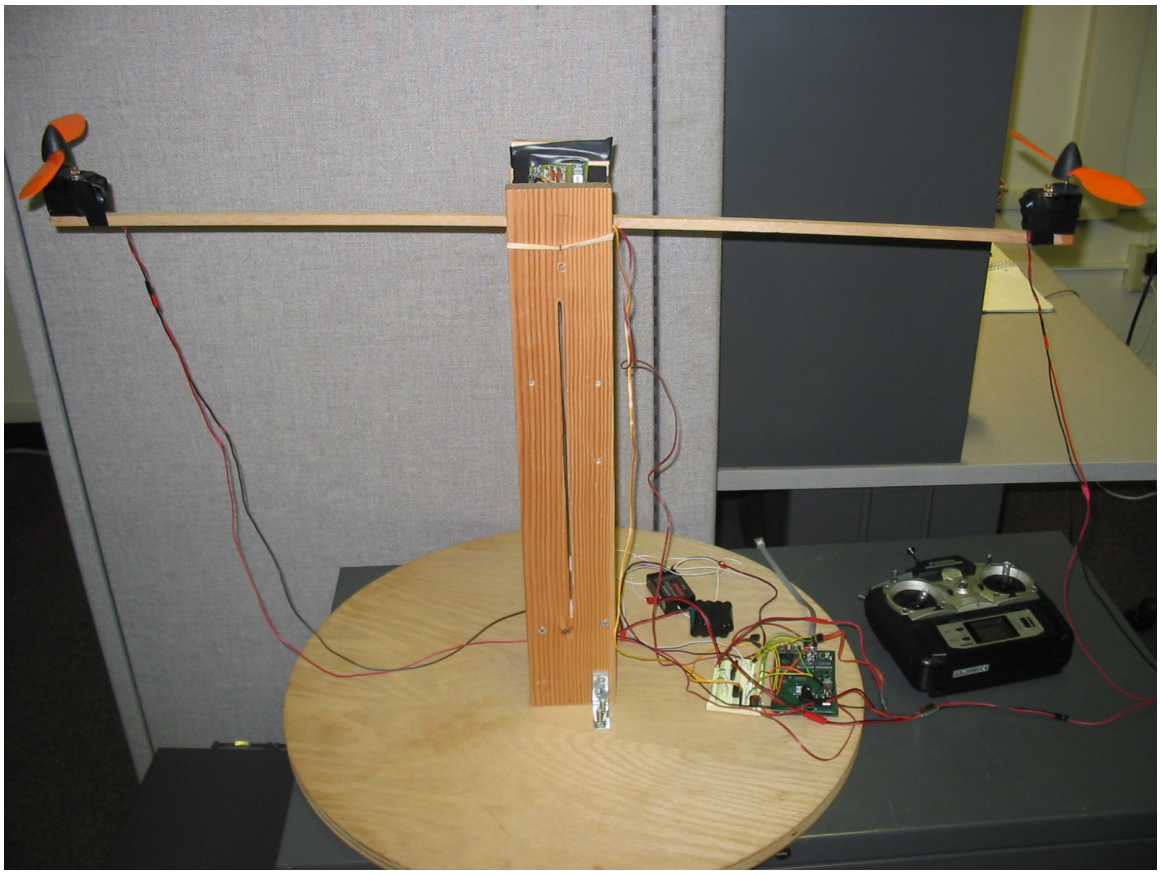

Figure 3.8. A picture of the setup used to develop and test the electronics for this project.

of a piece of wood that was constrained to rotate in one degree of freedom at its

midpoint. Pilot input from the R/C transmitter and receiver was converted into the desired angular velocity of the system and a desired thrust. The gyroscope described in section 3.3 was used to measure angular velocity and the PIC microcontroller was used to determine the motor output from the control law calculations that will be described in section 4.4.

3.10 Flight Data Recorder

An onboard flight data recorder from Eagle Tree Systems was used to record pilot inputs during tests using the two-rotor test system [54]. The data recorder can be used to monitor altitude, airspeed, battery level, and four channels of pilot controls. The flight data recorder is both lightweight and small: it weighs less than 3 ounces and its dimensions are 3.15 inches by 1.57 inches by 0.67 inches.

The flight data recorder is easily interfaced to a personal computer through a USB connection. An application is included with the recorder that is used to set the different recording options (parameters to be recorded, capture rate, etc.) for the flight data recorder. After the recorder has been used in flight, this application is needed to download the data from the recorder. The application can be used to view the recorded data and any error messages generated during the flight. The downloaded data can also be saved as a data file which can then be easily opened in Microsoft Excel or similar software.

The data capture rate is also adjustable and can be set to 5 different settings. The recorder automatically adjusts this rate depending on how fast the parameters that are being recorded are changing. When the airplane is performing turns or loops, the capture rate will be greater than when the airplane is stationary on

the ground. The default capture rate is 4 Hz, which is intended to give reasonable resolution and recording time. The recording time depends on the number of parameters being recorded, the capture rate, and how quickly the parameters change.

The flight data recorder was used to record the pilot inputs while using the test set-up. Although only two inputs were recorded, the flight data recorder can record up to four inputs. To record these inputs, "Y" cables must be installed between the radio receiver and the PIC microcontroller. The "Y" cables consist of three wires, ground, power, and input signal, similar to a standard servo cable and allow the pilot input to reach both the microcontroller and the flight data recorder. These cables allow the recorder to receive its power from the battery used to power the microcontroller.

3.11 Hardware Integration and Circuit Design

A circuit board was designed and fabricated to connect the PIC development board, gyroscopes, R/C receiver, battery, and electric speed controllers. Figure 3.9 shows a schematic of these connections. A freeware version (version 4.13) of the Eagle layout editor was used to create the circuit board, which is shown in figure 3.10 [55]. The software has a tool that allows circuit schematics to be created using the software library of parts as well as components created by the user. Once the schematic has been created, the parts can be placed on a circuit board using the board editor. The software program has an "auto-router" tool which places copper traces connecting the parts in the manner specified in the schematic. Files to send to a circuit fabrication shop for production of the circuit

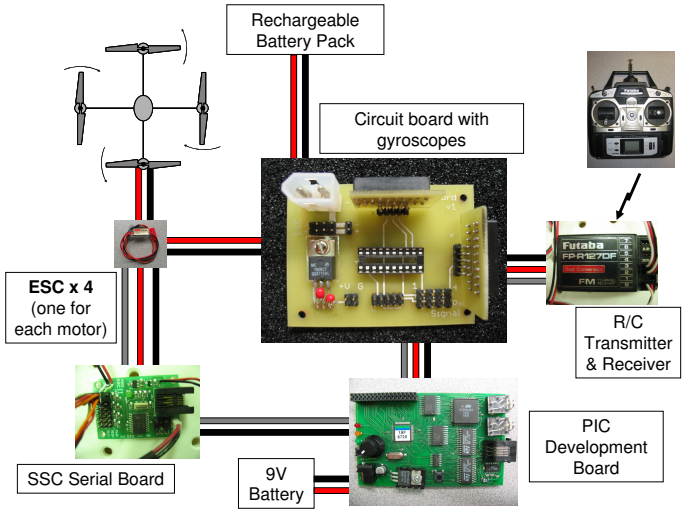

Figure 3.9. Schematic of the components connected using the fabricated circuit board.

board can also be made in this software program. The circuit board for the UAV was fabricated by Advanced Circuits at a cost of $40 [56].

The circuit board was designed so that three individual circuit boards were fabricated on a single board, which was cut using a band saw into the three smaller boards. The three circuit boards were needed so each of the three gyroscopes could measure angular velocity about a different perpendicular axis. Each of the three boards have holes for right angle male pin headers that permit the boards to be soldered onto the headers so that the three boards are perpendicular to each other.

A picture of the circuit before it was populated with gyroscopes and other cables and connectors is shown in figure 3.11. The two small boards are the two vertical boards in figure 3.11 and both hold a gyroscope. The large board is 2.25 inches by 3 inches and holds the following components:

Gyroscope A twenty pin dual inline socket was soldered to the board to hold the gyrscope evaluation board.

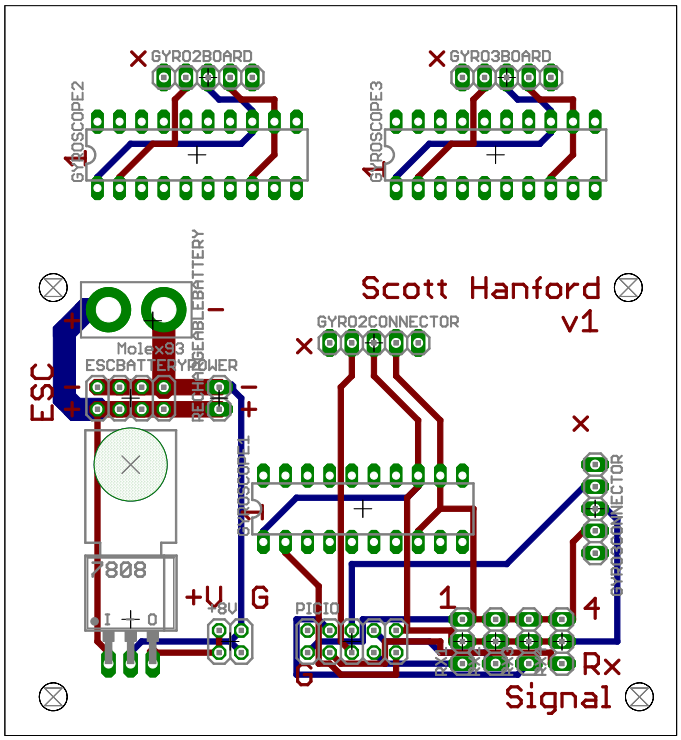

Figure 3.10. This picture shows the circuit board layout designed with the Eagle software program.

Connections to the two small boards For each of the two small circuit boards, five holes were placed for connecting the boards using single row, right angle male pin headers. The main circuit board was soldered to one end of the header and the small board was soldered to the other end, resulting in a right angle between the two soldered boards. The five holes and the header are used to connect the boards both electrically and mechanically. Two header

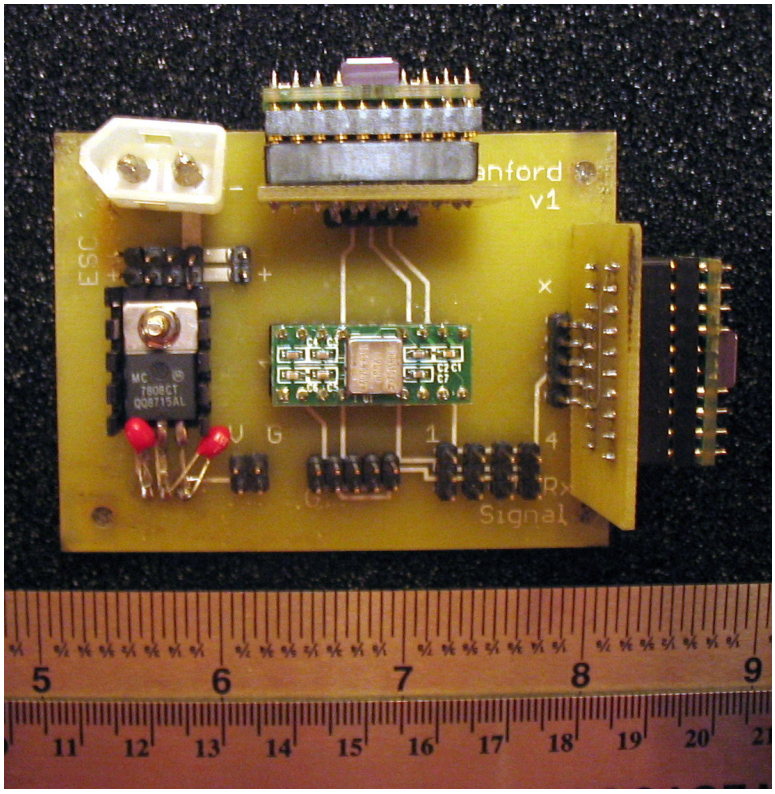

Figure 3.11. A picture of the main circuit board with the two small circuit boards attached at 90 degree angles. Two rulers are shown in this picture: the top ruler is in inches and the bottom ruler is in centimeters.

pins are used to supply the gyroscope on the small board with +5 volts and a ground. A third header pin carries the signal from the gyroscope to the main board. The two header pins that do not have electrical connections are used to strengthen the mechanical connection between the small and large boards.

R/C receiver Four single row straight male pin headers with three pins each were soldered onto the main circuit board to connect with the R/C receiver. The receiver can be connected to these headers using standard servo connectors (three pins: one signal, one ground, one positive voltage).

Connection with PIC development board A dual row straight male header was soldered to the main board to provide a connection from the main board to the PIC development board. Three pins were used for the gyroscopes, four pins were used for the R/C receiver input signals, and two pins were used for power and ground.

Battery and Power The main board was designed to power the quadrotor motors and the SSC board all with one battery. Two different types of connectors for powering the circuit boards were included in the design. A Molex^{TM} high current connection and a simple 0.1 inch pitch two pin header were included. Four single row straight male headers with two pins each provide the connections for powering the electric speed controllers from the battery. An eight volt regulator (7808) with 0.1 microfarad bypass capacitors is used to provide 8 volts to the PIC board.

3.12 Quadrotor frame

The main goals when designing and building the quadrotor frame were to create a frame that was lightweight but strong enough to survive rough landings and simple to build in case damage was sustained upon landing. The frame was made of two pieces of 3/8 inch by 3/8 inch square poplar. Each piece was 26 inches long. A notch was cut in the middle of each piece and the pieces were attached with epoxy to form a cross (figure 3.12). To attach the motors to the quadrotor frame, holes were drilled into a plastic mount that comes attached to the motors. These holes were drilled so that each end of the wood quadrotor frame could be slid into the

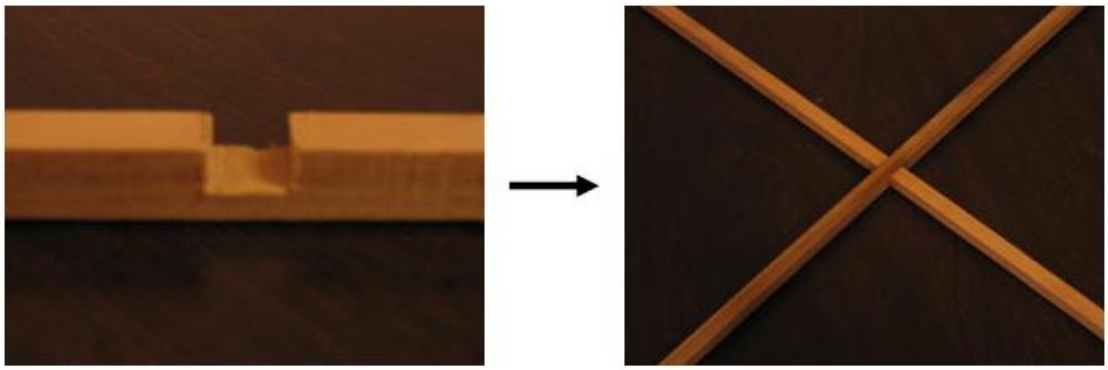

Figure 3.12. The picture on the left shows the notch that was cut into each piece of the cross. The picture on the right shows the two pieces of the cross after the notches have been placed together and the two pieces have been epoxied together.

holes. The motors were then secured by drilling small screws through both the plastic mount and the wood frame (figure 3.13).

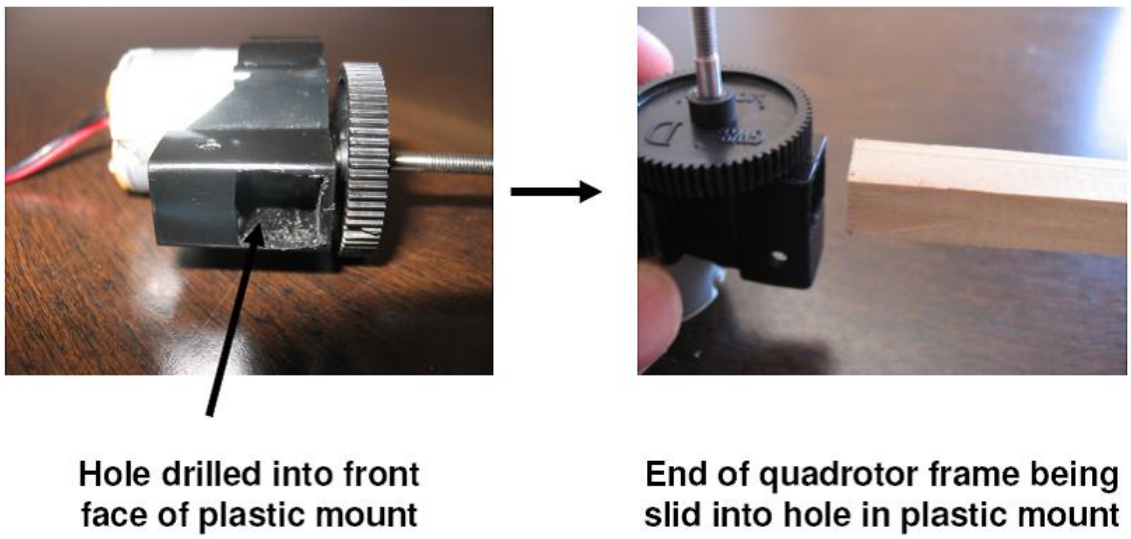

Figure 3.13. The picture on the left shows the hole that was drilled into the plastic mount of each motor. The picture on the right shows an end of the quadrotor frame being slid into the hole in the plastic mount. After the frame was slid into the hole in the plastic mount, small screws were used to secure the motor to the wood frame.

Lightweight, strong carbon fiber sheets from The Robot Marketplace [57] and half inch thick foam rubber were used to mount the electronics to the quadrotor

frame while isolating the sensors from vibrations in the frame. One carbon fiber sheet was attached to the top of the quadrotor frame using Dual Lock^{TM} fastener from 3M. Then the bottom of the foam rubber was fastened to this carbon fiber sheet and a second carbon fiber sheet was fastened to the top of the foam rubber. The electronics were fastened to the top of the second carbon fiber sheet, also using Dual Lock^{TM} fastener. The lithium polymer battery was attached to the bottom of the quadrotor frame using Dual Lock^{TM} fastener. To help protect the quadrotor frame and electronics during landings, additional pieces of poplar were attached to the frame to decrease the impact of landing on the quadrotor frame. The completed quadrotor is shown in figure 3.14.

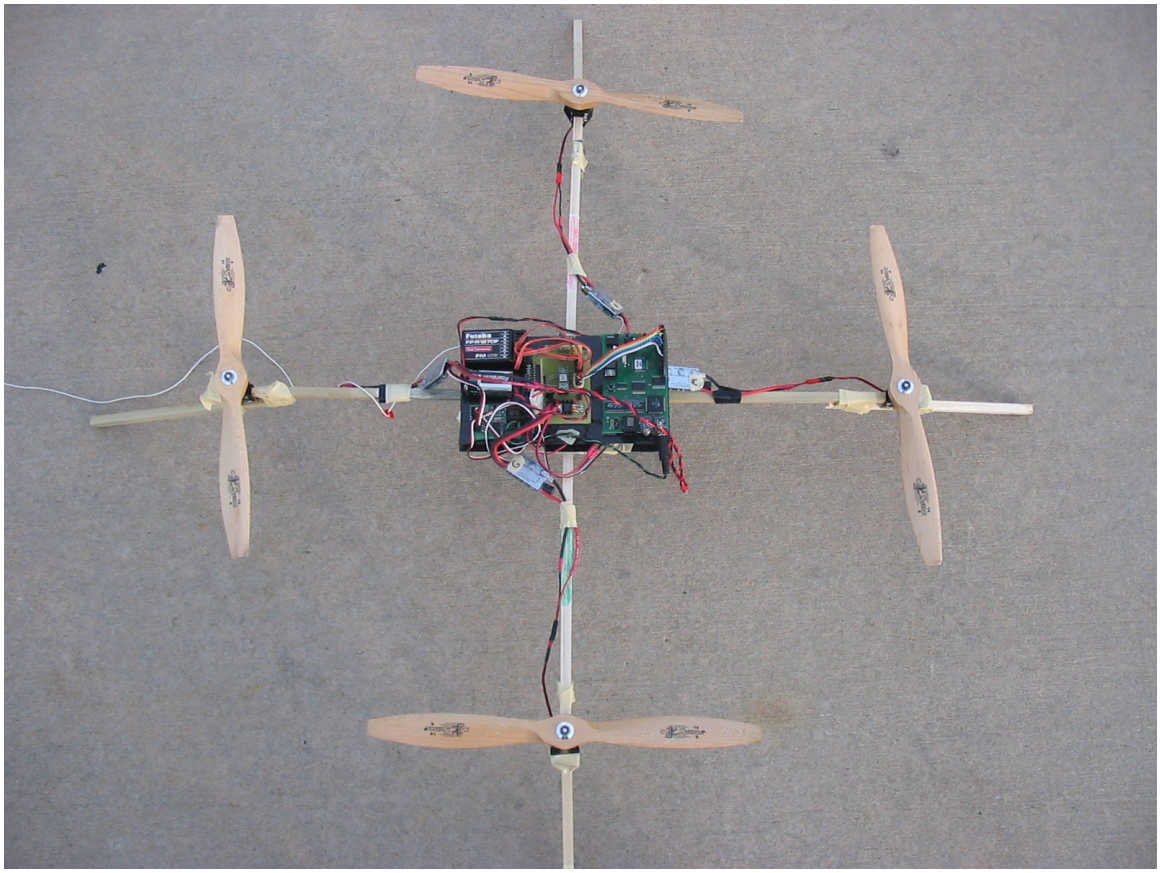

Figure 3.14. A picture of the completed quadrotor is shown.

Table 3.1 shows the costs of the individual components that were used to build the quadrotor. There a couple of ways to further reduce the cost of the quadrotor. Some of the prices shown in this table, particularly the custom-made circuit board, could be substantially lower if the components were purchased in larger quantities. A less expensive R/C transmitter and receiver could also be used. In addition, the PIC microcontroller and gyroscopes could be purchased in less expensive packages, as discussed in sections 3.2 and 3.3.

Table 3.1. This table lists the components used in the construction of the quadrotor, the price for each individual component, the number of components needed, and the total cost for each component. The total cost of the quadrotor was about $760.

Name of Component	Individual Cost ($)	Number Needed	Total Cost ($)
PIC Development Board	60	1	60
Gyroscope Evaluation Board	50	3	150
Electric Speed Controller	20	4	80
Motor/gearbox	10	4	40
Set of 2 Propellers	15	2	30
Propeller Adapter	5	4	20
R/C Transmitter & Receiver	180	1	180
SSC Board	60	1	60
Lithium Polymer Battery	85	1	85
Custom-made Circuit Board	40	1	40
Quadrotor Frame	15	1	15
Completed Quadrotor			760

Chapter 4

System Integration and Software

The software written to fly the quadrotor is described in this chapter. The features of the C compiler used to program the PIC microcontroller and the interfaces to each piece of hardware are discussed. The structure of the program written to fly the quadrotor and the characteristics of the control law used in this program are then explained.

4.1 CCS C compiler

CCS, Inc. has developed a C compiler called the PCWH for the PIC 18F8720 microcontroller [45]. This compiler is easy to use with CCS's Windows based IDE (integrated development environment) and its "C aware" editor. This editor highlights C syntax features with colors, has tab control, can search for matching brackets or parentheses, and has other features. This is not an ANSI compliant C compiler and it has some differences from a traditional C compiler because of separate code and data segments in the PIC hardware. This compiler does have some of the standard ANSI library and math functions and has many extensions

that are useful when working with the PIC hardware. The compiler has built-in libraries for working with RS-232 serial input and output, digital input and output, and precision delays and makes hardware features such as timers and A/D conversion easy to use with C functions. In addition to 1, 8, 16, and 32 bit integer types, 32 bit floating point numbers and floating point math, which is very important for the control calculations used in this research, are also supported.

The IDE and compiler allow viewing of C and assembly code side by side and insertion of assembly code that may reference C variables anywhere in the source code. The compiler also comes with many ready to run example C programs written for the PIC 18F8720 microcontroller that demonstrate how some built-in functions can be used.

4.2 System Integration

This section describes the C code that was written to interface the PIC microcontroller with the hardware used in this project.

4.2.1 Gyroscope and A/D Converter

The 10 bit analog to digital converter was used to convert the output voltage from the gyroscope that represents angular velocity to an integer between 0 and 1023. An interrupt service routine (ISR) and a timer on the PIC (timer4) were used to sample each of the three gyroscopes (yaw, pitch, and roll) every millisecond. The readings for each individual gyroscope were then averaged in the main control loop, which is executed every 20 ms. Timer4 was set to overflow every millisecond and

to cause an interrupt when each overflow occurred. The code inside the ISR that was executed at each interrupt is shown in figure 4.1. As shown in the figure, an A/D conversion for the current gyroscope is performed, the 10 bit value from the conversion is added to a variable that stores the sum of the current gyroscope's readings (pitchGyroReadings, for the gyroscope that measures pitch rate), and a counter to keep track of the number of readings obtained for the current gyroscope (pitchNumGyroReadings, for example) is incremented. Then, the channel to be used for the next A/D conversion is set. When the results for each gyroscope are averaged in the control loop, the variables that store the sum and the number of the gyroscope readings are reset to zero so the variables will be ready for the next iteration of the control loop.

4.2.2 R/C receiver and Capture/Compare/Pulse width modulation channels

The capture/compare/pulse width modulation (CCP) hardware was set to capture mode to obtain four inputs from the R/C receiver by measuring the pulse lengths from the receiver. Each input channel to be read from the receiver has three pins, as described in section 3.5. The positive voltage and reference ground pins were connected to the PIC positive voltage (+5 volts) and the PIC reference ground. The signal from each channel was connected to one of the CCP pins on the PIC microcontroller.

Although all of the CCP pins can measure pulse lengths simultaneously, this would require a timer to be used for each individual CCP pin. Since four CCP pins are used to measure pulse lengths from the R/C receiver, four out of the five

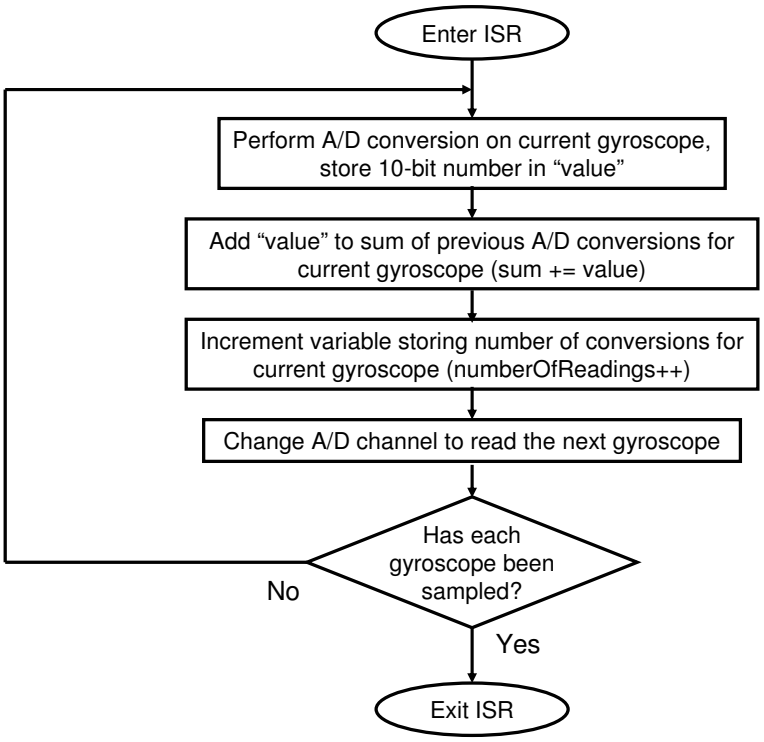
Enter ISR
Perform A/D conversion on current gyroscope, store 10-bit number in "value"
Add "value" to sum of previous A/D conversions for current gyroscope (sum += value)
Increment variable storing number of conversions for current gyroscope (numberOfReadings++)
Change A/D channel to read the next gyroscope
Has each gyroscope been sampled?
No
Yes
Exit ISR

Figure 4.1. A flowchart describing the interrupt service routine used to sample the gyroscope.

timers on the PIC microcontroller would need to be used. To avoid this situation and leave timers available for other tasks, an algorithm was written to record one input pulse at a time using only one timer (timer1). The four input pulses are read consecutively (pitch, thrust, roll, and yaw) and then this order is repeated continuously. An interrupt service routine (ISR) was written for each CCP pin. Figure 4.2 shows a flowchart illustrating the structure of the code written in each ISR.

In capture mode the CCP hardware can be configured to cause an interrupt on either the rising or falling edge of a pulse. When the rising or falling edge

occurs, the current value of the timer being used with the CCP pin is copied to a 16 bit integer unique to the current CCP pin. A simple method to measure a pulse length is to configure the CCP hardware to cause an interrupt on a rising edge. In the interrupt service routine for this CCP pin, the timer value at the time of the interrupt that was copied to the 16 bit integer for the current CCP pin can be saved as a variable ("riseTime," for example), the CCP hardware can be configured to cause an interrupt on a falling edge, and a flag can be set to indicate that the rising pulse edge has occurred. When the falling edge occurs and causes an interrupt, the value of the timer is copied into a 16 bit integer as described above. The variable "fallTime" can be set equal to this value. The value of "fallTime" minus the value of the variable "riseTime" will be equal to the length of the pulse in CPU ticks. Since the PIC is run at a processing speed of 20 MHz, five CPU ticks correspond to 1 microsecond. This technique can be used to determine the amount of time that any digital pulse is high or low.

4.2.3 Serial Servo Controller and serial communication

As described in section 3.6, the Serial Servo Controller must receive a three byte sequence to send a servo pulse [48]. The pins on the PIC through which the serial data is sent and the baud rate at which the data is to be sent are defined in the C program. A function called "serialOut" was written to send the three bytes sequences to the SSC through one of the serial ports on the PIC development board. The serialOut function uses the C command "putc" to accomplish the serial communication. There are two arguments that must be passed to this function: the number of the motor the data should be sent to and the desired length of the

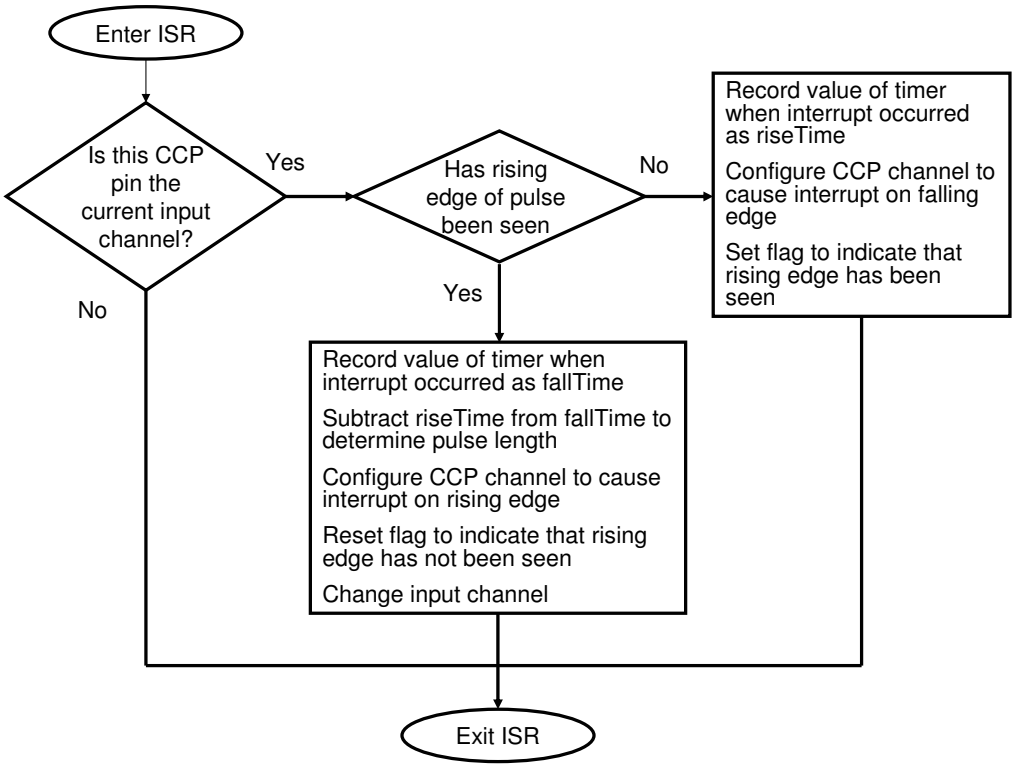
Enter ISR
Is this CCP pin the current input channel?
Yes
No
Has rising edge of pulse been seen
No
Yes
Record value of timer when interrupt occurred as riseTime
Configure CCP channel to cause interrupt on falling edge
Set flag to indicate that rising edge has been seen
Record value of timer when interrupt occurred as fallTime
Subtract riseTime from fallTime to determine pulse length
Configure CCP channel to cause interrupt on rising edge
Reset flag to indicate that rising edge has not been seen
Change input channel
Exit ISR

Figure 4.2. A flowchart describing the interrupt service routine used to measure the length of one input pulse from the R/C receiver.

servo pulse.

4.3 Program structure

Figure 4.3 is a flowchart of the body of the program used to control the quadrotor vehicle. The first part of the program declares all of the variables needed throughout the program as well as variables that were used for troubleshooting during code development and for storing results during quadrotor flights. The serialOut function and interrupt service routines (for timer1, timer3, each of the four CCP

channels, and timer4 for gyro reading) are then defined. The serialOut function is then used to arm the ESCs by sending 1 ms long servo pulses to all the ESCs for one second. Next, the CCP channels, timers, and A/D converter are set up and the interrupts are enabled. For the next five seconds, each of the three gyroscopes are sampled while the quadrotor is stationary to determine the reading for each gyroscope when there is zero angular velocity.

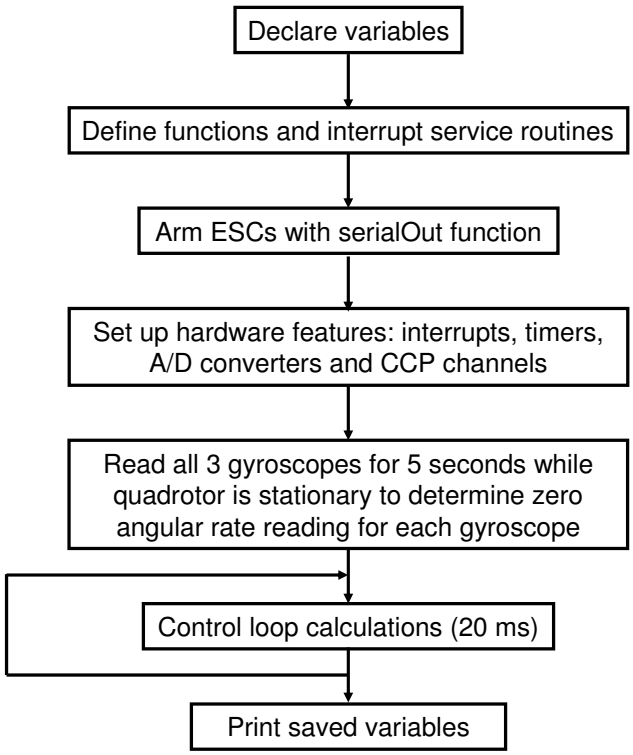
Declare variables
Define functions and interrupt service routines
Arm ESCs with serialOut function
Set up hardware features: interrupts, timers, A/D converters and CCP channels
Read all 3 gyroscopes for 5 seconds while quadrotor is stationary to determine zero angular rate reading for each gyroscope
Control loop calculations (20 ms)
Print saved variables

Figure 4.3. A flowchart showing the entire program structure.

The control loop is the next part of the program. This loop executes until a button on the PIC development board is pressed. The control loop is designated to be 20 ms long. Once the code in the control loop has been executed, the loop

timer is repeatedly checked until 20 ms have passed. The next iteration of the loop is then started. The servo pulses from the SSC board are sent every 20 ms, so updating their length more often than 20 ms is unneccesary. The time spent waiting for 20 ms to pass before starting the loop's next iteration could be used to communicate with additional sensors or perform additional calculations. Once the button to exit the control loop is pressed, the serialOut function is used to turn the motors off and the variables that have been saved during the program execution are printed to a computer monitor.

4.4 Control loop

The structure of the control loop is given in figure 4.4. For each iteration of the control loop, the current angular rates and pilot inputs are determined, the control calculations are performed, and signals are sent to the motors.

4.4.1 Determining angular rates

First, the sum of the gyroscope readings since the last iteration of the control loop is divided by the number of readings since the last iteration of the control loop to find the average angular velocity over the last 20 ms. This calculation is repeated for all three gyroscopes. The variables storing the sum of the gyroscope readings and the number of gyroscope readings then must be reset to zero for all three gyroscopes.

The angular rates are then obtained using equation 4.1.

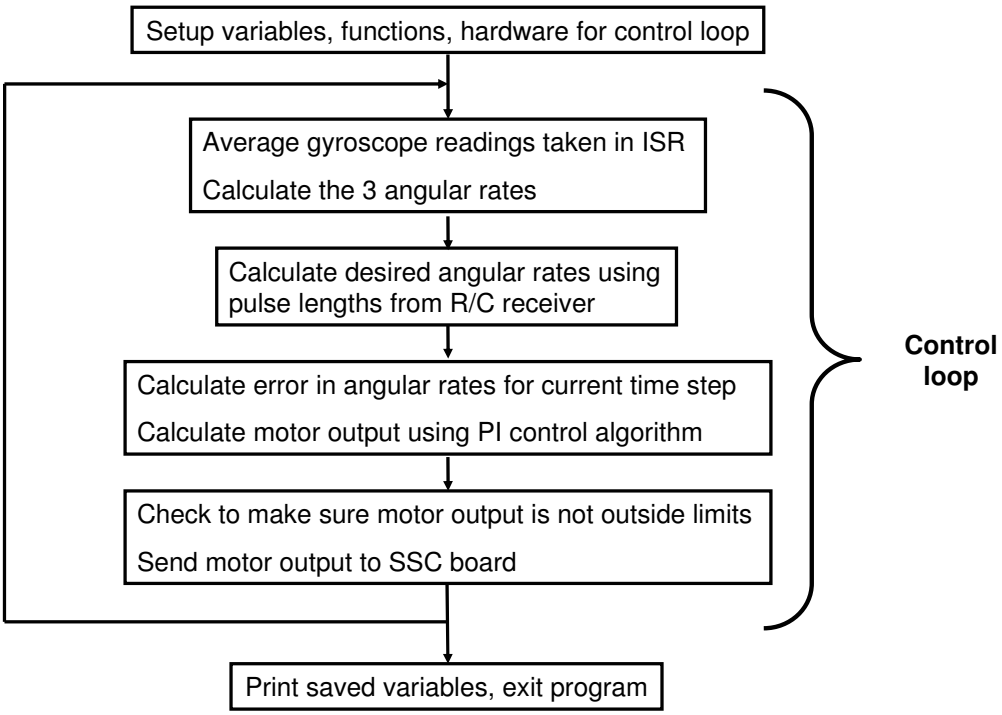
Setup variables, functions, hardware for control loop
Average gyroscope readings taken in ISR
Calculate the 3 angular rates
Calculate desired angular rates using
pulse lengths from R/C receiver
Calculate error in angular rates for current time step
Calculate motor output using PI control algorithm
Check to make sure motor output is not outside limits
Send motor output to SSC board
Print saved variables, exit program
Control
loop

Figure 4.4. A flowchart describing the steps used in the control loop.

$$\text{Angular velocity} = \frac{\frac{5}{1023}(\text{average gyro reading} - \text{zero gyro reading})}{0.0125} \tag{4.1}$$

The value of the gyroscope reading when there is zero angular velocity is subtracted from the average gyroscope reading that was just calculated. This difference in gyroscope readings is multiplied by 5 (the output from the gyroscope is 0–5 volts) and divided by 1023 (the A/D conversion is 10 bit so the range of the result is 0–1023). This number is then divided by 0.0125 because the gyroscope output signal changes by 12.5 milliVolts for a change in angular velocity of one degree per

second.

4.4.2 Determining pilot inputs

The pilot inputs are then calculated using the length of pulses from the R/C receiver determined using the CCP channel interrupt service routine (ISR) described earlier in section 4.2.2. Equation 4.2 is used to convert the measured pulse lengths to the desired angular rates.

$$\omega_d = \text{Input gain} * \left(\frac{\text{Input pulse length}}{5} - 1500 \right) \tag{4.2}$$

The pulse lengths measured by the CCP channel ISRs are in microcontroller ticks, which must be divided by 5 to get the pulse lengths in microseconds. The three sticks on the R/C transmitter corresponding to the three angular rates of the quadrotor are spring-loaded and rest in the middle of their range. This means that with no input applied to the sticks, the pulses from these three channels are about 1500 microseconds (μs) long. Fifteen hundred μs are subtracted from the length of the pulse in microseconds so that when no force is applied to the sticks on the transmitter the desired angular rates are zero. To ensure that the range of possible desired angular rates corresponds to most of the range of measured angular rates (150 degrees per second), the input gain was set to 0.1. This means that when the transmitter stick is pressed to its positive limit, the pulse length will be about 2000 μs and the desired angular velocity will be about 100 degrees per second. When the transmitter stick is pressed to its negative limit, the pulse length will be about 1000 μs and the desired angular velocity will be about -100 degrees per second. This input gain can also be decreased to give more sensitivity

for a smaller range of desired angular rates.

4.4.3 PI control law

A proportional and integral (PI) control law is used to calculate motor outputs to minimize the error between each of the quadrotor's three desired angular rates and the measured angular rates. The error for each of the three angular rates is calculated by subtracting the measured angular velocity that was calculated from the gyroscope readings from the desired angular velocity, determined from the pilot inputs. The proportional term of the controller produces a signal proportional to the error in angular rate. Increasing the effect of this term, which is accomplished by increasing the gain (kP) associated with this term, decreases the response time of the system being controlled. Increasing the gain too much can have an adverse effect on the stability of the system. The integral term of the controller results in a signal that is proportional to the integral of the error in angular rate. This term can be used to eliminate steady state error in angular rate. Increasing the gain (kI) associated with this term too much can lead to oscillations of the system about its desired angular rate [58].

Figure 4.5 shows a block diagram of a system with a PI controller, intended to represent the control of one of the three angular rates of the quadrotor. The input signal (r) respresents the input from a pilot. This input is converted into a desired angular rate, ω_d. A summing junction subtracts the measured angular rate, ω_m, from the desired angular rate to determine the error e (equation 4.3). The measured angular rate is calculated from the gyroscope output (y) as described in equation 4.1.

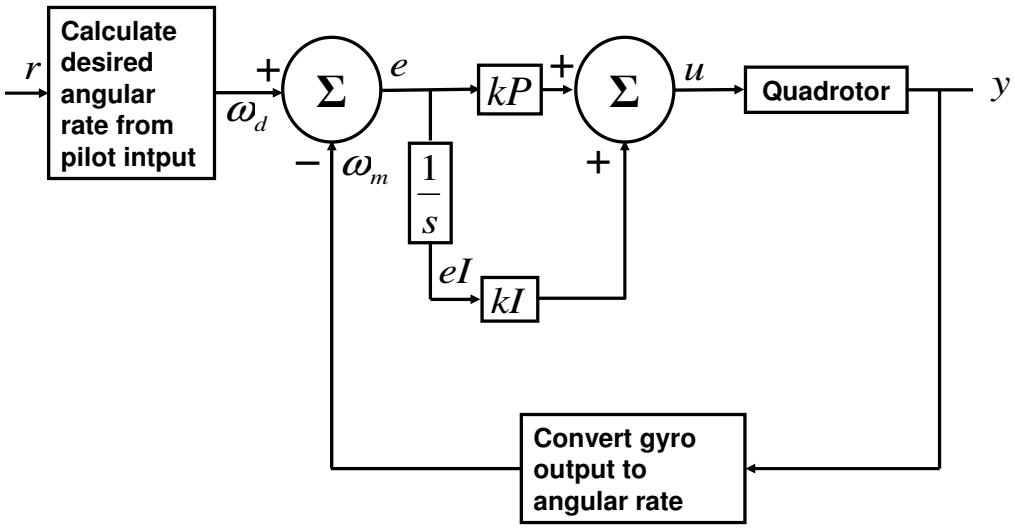

Figure 4.5. A block diagram describing a system with a PI controller.

$$\mathrm{e} = \omega_d - \omega_m \tag{4.3}$$

The integral of the error (eI) is then found by adding the product of the current error and the current time step to the integral of the error calculated at the previous timestep (equation 4.4). The integral of the error could also by found using more accurate numerical integration techniques, such as trapezoidal integration, with a minimal increase in computation time.

$$\mathrm{eI} = \mathrm{eI} + \mathrm{timeStep} * \mathrm{e} \tag{4.4}$$

This integral is represented by the $\frac{1}{s}$ term in figure 4.5. The PI controller uses the proportional (kP) and integral (kI) gains, the current error (e), and the integral of the error (eI) to calculate the motor outputs (u), as described in equation 4.5.

$$u = \mathrm{kP} * \mathrm{e} + \mathrm{kI} * \mathrm{eI} \tag{4.5}$$

A motor output is calculated for each of the three angular rates (uPitch, uRoll, and uYaw) using equation 4.5 and for the collective thrust (uThrust) using the pilot input for thrust.

4.4.4 Driving the motors

As described in section 2.1, the command to be sent to each motor (u1 for motor 1, u2 for motor 2, u3 for motor 3, and u4 for motor 4) is a combination of the collective thrust (uThrust) and the motor outputs for the three angular rates (uPitch, uRoll, and uYaw). Equations 4.6–4.9 are used to calculated the value of the output to send to each motor.

$$\mathrm{uMotor1} = \mathrm{uThrust} - \mathrm{uPitch} + \mathrm{uYaw} \tag{4.6}$$

$$\mathrm{uMotor2} = \mathrm{uThrust} + \mathrm{uRoll} - \mathrm{uYaw} \tag{4.7}$$

$$\mathrm{uMotor3} = \mathrm{uThrust} + \mathrm{uPitch} + \mathrm{uYaw} \tag{4.8}$$

$$\mathrm{uMotor4} = \mathrm{uThrust} - \mathrm{uRoll} - \mathrm{uYaw} \tag{4.9}$$

The final step in the control loop is to check to make sure the outputs that will

be sent to the motors (u1–u4) are within the range of values that are acceptable to the SSC board. The serialOut function, described in section 4.2.3, is then used to send the motor commands to the SSC board.

Chapter 5

Results

This chapter gives results from the test system, tests of the control law implementation, and flights of the quadrotor.

5.1 Test System

The electronics and PI control law were tested using the two-rotor system described in section 3.9. Two pilot inputs from the R/C transmitter and receiver were used to determine the desired thrust and pitch rate. A gyroscope was mounted on the test system to measure the pitch rate. The PI control law was used to calculate the speed of the two motors needed to maintain the desired angular velocity of the system. The proportional and integral gains in equation 4.5 were tuned experimentally so that the test system exhibited a satisfactory response to disturbances.

To show the importance of using feedback from the gyroscope, tests were performed to try to keep the test system level both with and without pitch rate feedback from the gyroscope. The Flight Data Recorder described in section 3.10

was used to record the pilot input for pitch rate in both cases and outputs from the gyroscope were saved in the PIC microcontroller's RAM and printed to a computer monitor after the tests.

Figure 5.1 shows the pitch rates that were recorded by the gyroscope during these tests. The pitch rates recorded during the test without feedback control had a much higher range, from −80 to +80 degrees per second, than the pitch rates for the test with feedback control, which had a range of −20 to +20 degrees per second.

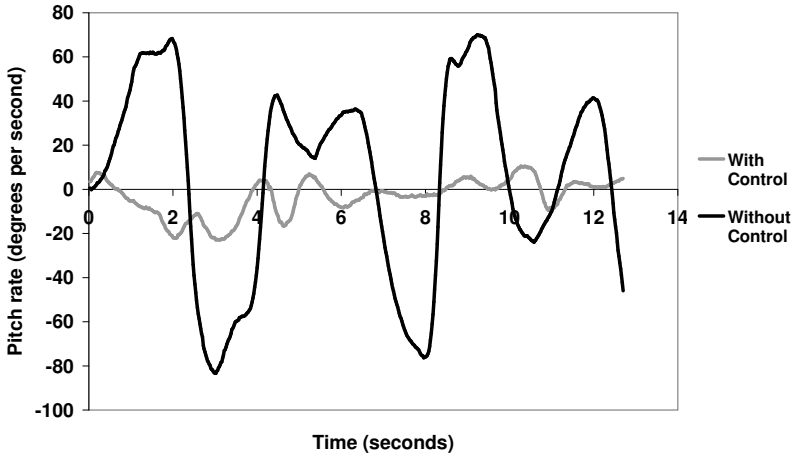

Figure 5.1. This graph shows the pitch rate of the test system during tests both with (gray) and without (black) control feedback.

Figure 5.2 shows the pilot inputs for pitch rate, recorded using the Flight Data Recorder, throughout the two tests. A desired pitch rate of zero degrees per second means that the transmitter stick is in its middle position, indicating no force on the

stick from the pilot. This means that the pilot was was not giving any adjustments to the desired pitch rate at that moment.

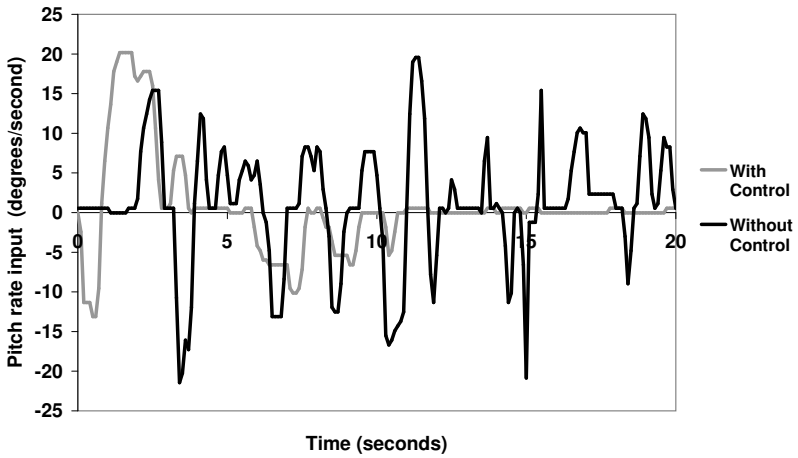

Figure 5.2. This graph shows the pilot inputs for pitch rate of the test system during tests both with (gray) and without (black) control feedback.

In addition to the smaller range of pitch rate measured during the test with feedback, less pilot input was needed, especially after the first 11 seconds of the test. Even during the first 11 seconds of the test that used feedback, the changes to the pilot input were smooth and gradual. Throughout the test without feedback, the pilot input was constantly adjusted.

5.2 PI Control Law

Tests were performed to show the results of the control law calculations for pitch, roll and yaw rotations. Rotations of the quadrotor were performed manually. The angular rates measured using the gyroscope and the motor outputs calculated from the control law (equations 4.6–4.9) were recorded throughout the tests for these rotations. The desired angular rates for each axis (pitch, roll, and yaw) were equal to zero throughout these tests so any rotation resulted in an error with a magnitude equal to the magnitude of the measured rotation. The motors were not connected during these tests so any rotations of the quadrotor were a result of the manual rotations.

The results obtained during the test of the PI control law for the pitch direction are shown in figure 5.3. The differential motor output in the pitch axis was defined as the output to motor three minus the output to motor one. At the beginning of the test, the pitch rotation and error in pitch rate are equal to zero and the differential motor output is also zero. A little after two seconds into the test, the quadrotor frame was rotated about its pitch axis. This pitch rotation caused the pitch gyroscope to sense an angular rotation, resulting in an error in pitch rate. The control law calculations then increased the output to motor three and decreased the output to motor one, in an attempt to minimize the error in pitch rate. Figure 5.3 shows the differential motor output for the motors on the pitch axis increasing during the pitch rotation. After the pitch rate and error return to zero (shortly before four seconds), the effect of the integral term in the PI control law can be seen. Although the error in pitch rate was very close to zero, the integral of the pitch error was not zero because the integration of the previous pitch error was

greater than zero. Therefore, a difference in the two motor outputs remained.

Similar results were obtained for the test of roll rotations (figure 5.4). The quadrotor frame was briefly rotated about its roll axis (first in the negative direction for a very short amount of time and then in the positive direction). For this test, the differential motor output was defined as the output to motor two minus the output to motor four. The large positive roll rates caused the control law to increase the differential motor output between the motors in the roll axis. The effect of the integral term can again be seen after the roll rate error becomes very close to zero.

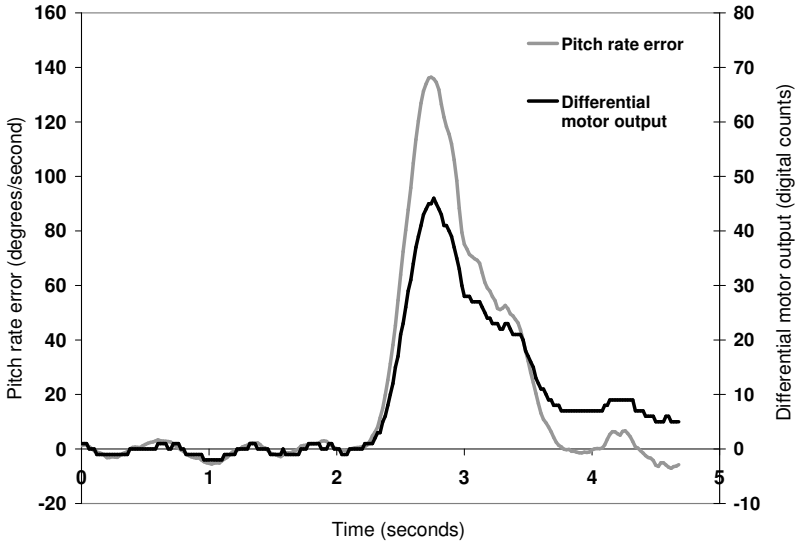

Figure 5.3. This graph shows the pitch rate (gray) of the quadrotor in degrees per second and the differential motor output in digital counts for the pitch axis (black) calculated during a test of the control system. The scale for the error in pitch rate is shown on the vertical axis on the left and the scale for the differential motor output is shown on the vertical axis on the right.

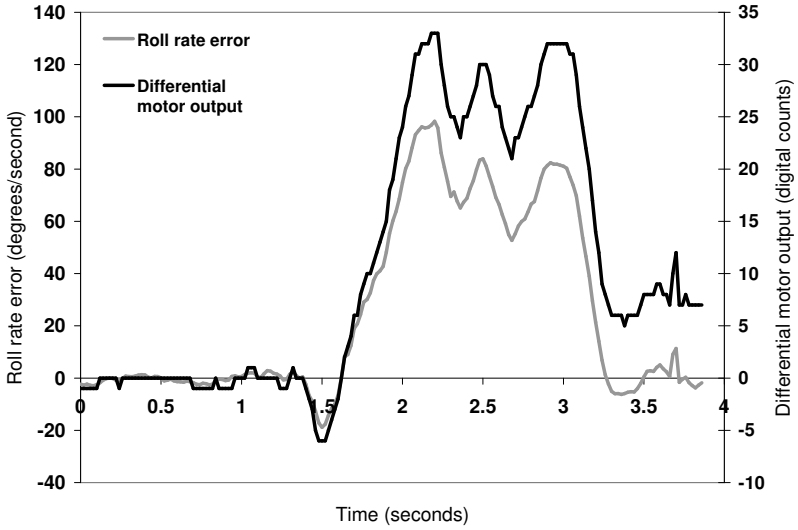

Figure 5.4. This graph shows the roll rate (gray) of the quadrotor in degrees per second and the differential motor output in digital counts for the roll axis (black) calculated during a test of the control system. The scale for the error in roll rate is shown on the vertical axis on the left and the scale for the differential motor output is shown on the vertical axis on the right.

The results for the test of the control law for rotation about the yaw axis are shown in figure 5.5. The differential motor output for this test was defined as the output to the counter-clockwise-rotating motors (motors one and three) minus the output to the clockwise-rotating motors (motors two and four). One and a half seconds into the test, the quadrotor was rotated about its yaw axis and the control law increased the differential motor output between the counter-clockwise rotating and clockwise rotating motors. After the yaw rotation decreased to zero (at four and one half seconds), the differential motor output remained non-zero because of the integral term in the PI control law.

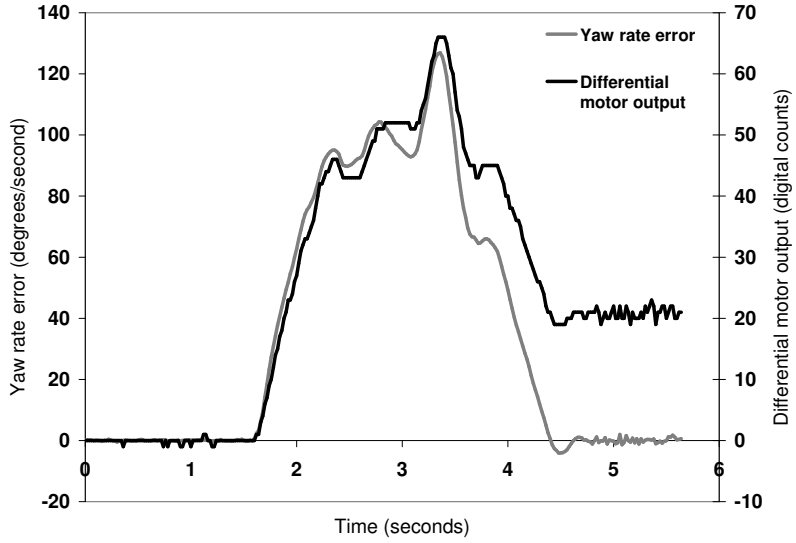

Figure 5.5. This graph shows the yaw rate (gray) of the quadrotor in degrees per second and the differential motor output in digital counts (black) for the yaw axis calculated during a test of the control system. The scale for the error in yaw rate is shown on the vertical axis on the left and the scale for the differential motor output is shown on the vertical axis on the right.

5.3 Quadrotor flights

Several quadrotor flights were successful. An inexperienced R/C pilot was able to command the quadrotor to lift off the ground using only thrust input, keep the quadrotor in the air above a fairly small area (15 feet by 15 feet) by providing pitch, roll, and yaw inputs, and gently land the quadrotor. Although flight times were short (< 20 seconds), a more experienced R/C pilot is likely to be able to increase the lengths of these flights easily. For the first few tests, the proportional and integral gains for the pitch and roll axes were set equal to the gains used for the test system. These gains were then adjusted after each flight to make the

quadrotor easier to fly. Since the quadrotor dynamics of the pitch and roll axes are similar, the gains for these axes are similar in magnitude. The proportional and integral gains for the yaw axis were harder to tune and were adjusted after flights during which control of the yaw rate was not satisfactory. Pictures of the quadrotor in flight are shown in figures 5.6 and 5.7.

Figure 5.6. A side-view of the quadrotor in flight.

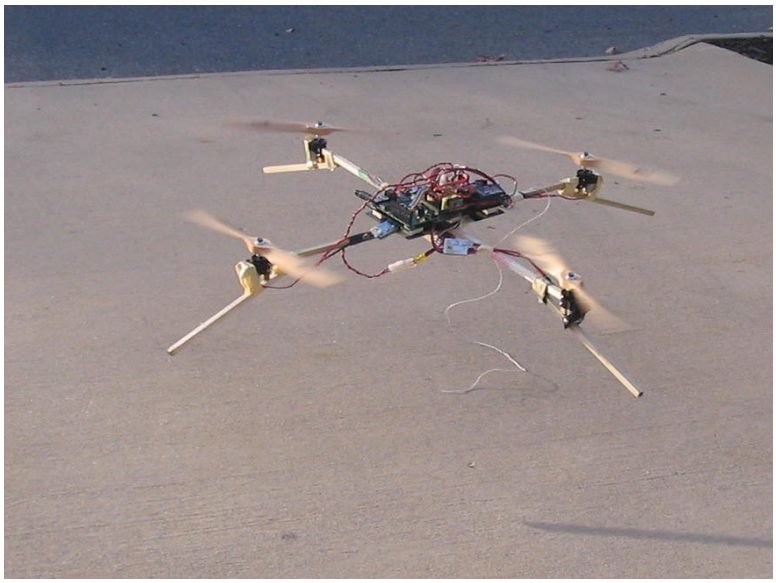

Figure 5.7. Another picture of the quadrotor in flight.

5.3.1 Pitch rate and input during a flight

Figure 5.8 shows the pitch rates of the quadrotor and the pilot inputs for pitch rate stored in the microcontroller's RAM on the quadrotor during a flight. The quadrotor began to rotate in the negative pitch direction a little under seven seconds into the test. Shortly after the rotation begins, the pilot gave two inputs (first a shorter input and then a longer one) in response to the pitch rotation. This pilot input and the control law created a differential motor output to the motors on the pitch axis (motors one and three) that resulted in a decrease in the magnitude of the negative pitch rotation about seven seconds into the test. A little after seven seconds into the flight, the pilot also decreased the input for thrust, causing the quadrotor to land on the ground about eight seconds into the test, causing the large spike in pitch rate seen at eight seconds.

5.3.2 Angular rates during a flight

The yaw, pitch and roll rates of the quadrotor were stored in the microcontroller's RAM during another flight. At the completion of the flight, these rates were printed to a computer monitor using the PIC development board's serial port. The three rates recorded during this quadrotor flight are shown in figures 5.9–5.11. The quadrotor lifted off the ground about five seconds into the test and landed on the ground a little after ten seconds into the test. The rates during landing were not recorded because the microcontroller on the quadrotor ran out of memory to store the angular rates shortly before landing occurred. During this flight, the quadrotor lifted off the ground while tilted in its pitch and roll axes and flew in the direction of its tilt until pilot input was given to correct for this tilt. The

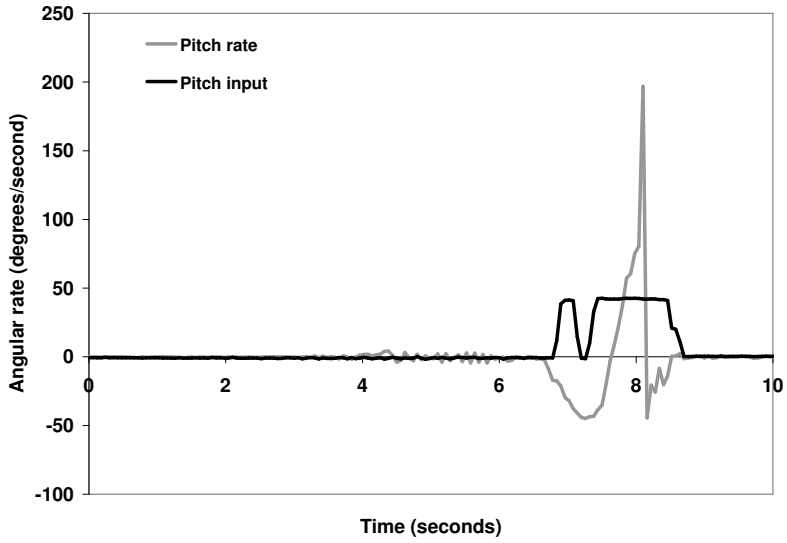

Figure 5.8. The pitch rate (gray) and pilot input for pitch rate (black) during a quadrotor flight are shown.

quadrotor then remained over a stationary point on the ground while its pitch and roll rates oscillated around zero. The quadrotor also rotated about its yaw axis while hovering over this stationary point. The pilot then reduced the thrust input and the quadrotor landed. The quadrotor stayed within three feet of the ground during this flight. Since the quadrotor flew so close to the ground, there may have been some attitude stabilization from ground effect that would not have been present for a flight at a greater height above the ground.

Figure 5.9 shows the pitch rate of the quadrotor during this flight. The quadrotor motors were turned on about one and a half seconds into the test when the small oscillations in pitch rate started. After the quadrotor lifted off the ground at a time of about five seconds, there was a positive pitch rate for a short amount

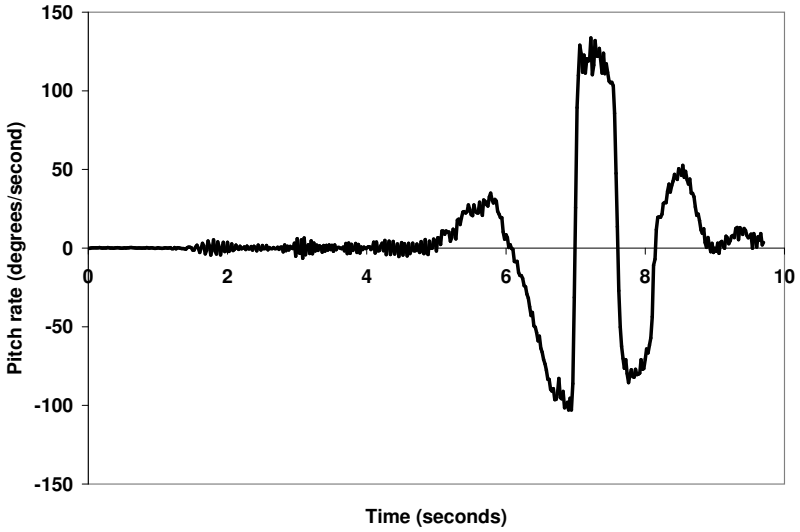

Figure 5.9. A graph showing the pitch rate in degrees per second of the quadrotor during a flight.

of time. Between six and seven seconds into the test, the quadrotor experienced a negative pitch rate and the pilot gave an input to increase the pitch rate. This input caused the pitch rate to reach a peak magnitude of about 130 degrees per second seven seconds into the test, but the PI control law decreased this high pitch rate by the time the quadrotor landed.

The roll rate during this flight is shown in figure 5.10. After the quadrotor lifted off of the ground five seconds into the test, the quadrotor experienced a brief positive roll rate and then a larger negative pitch rate. Between six and seven seconds into the test, the pilot gave an input to increase the roll rate. Similar to the input for pitch rate, this roll input resulted in a peak magnitude of roll rate (about 120 degrees per second). The roll rate also decreased by the time the

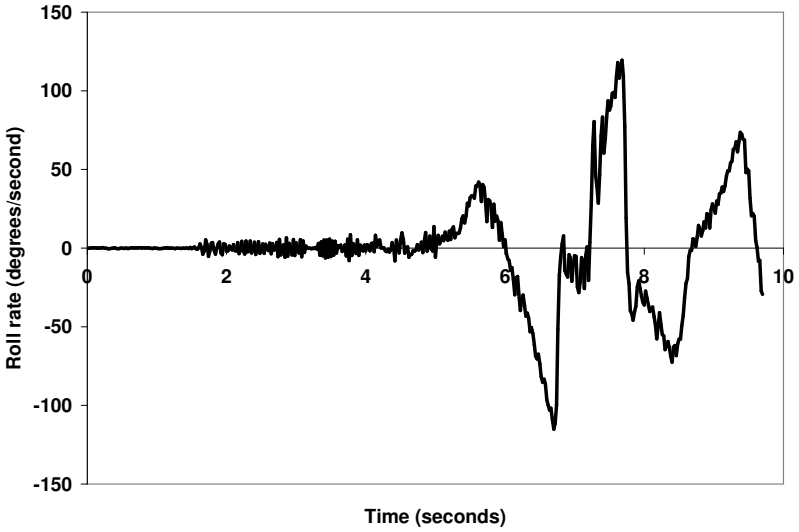

Figure 5.10. A graph showing the roll rate (in degrees per second) of the quadrotor during a flight.

quadrotor landed.

Figure 5.11 shows the yaw rate of the quadrotor during this flight. The magnitude of the yaw rate stayed relatively small (< 20 degrees per second) during the first two seconds of the flight (between five and seven seconds of the test). Then the yaw rate increased and had a large magnitude for most of the rest of the test. The yaw rate is controlled by the moment created by the difference in propeller torques between the counter-clockwise rotating and clockwise rotating motors while the pitch and roll rates are controlled by the moment resulting from the difference in propeller thrusts between the two motors on the pitch and roll axes. The yaw rate can be more difficult to control than the pitch and roll rates because the moment created by the difference in propeller torques is smaller in magnitude than

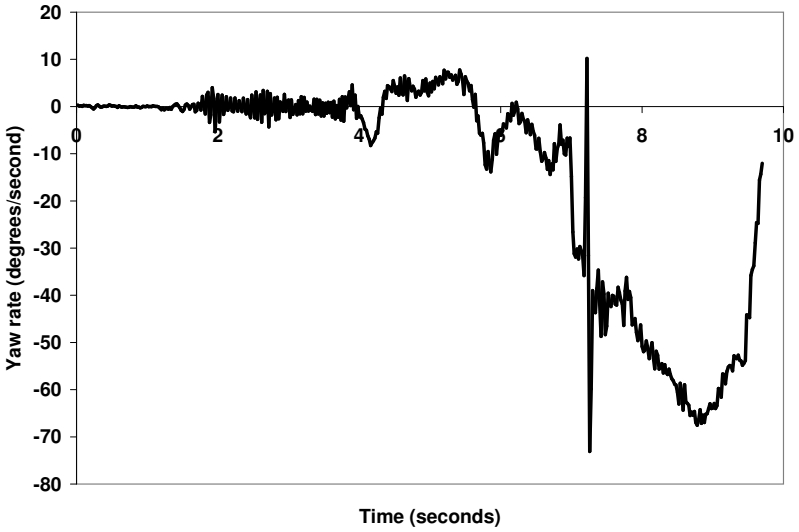

Figure 5.11. A graph showing the yaw rate (in degrees per second) of the quadrotor during a flight.

the moment created by the difference in propeller thrusts, resulting in less control authority for the yaw rate than for the pitch and roll rates.

5.3.3 Euler angles during a flight

Using the angular rates saved during the same quadrotor flight that was described in section 5.3.2, the Euler angles of the quadrotor were calculated after the flight using equations 5.1–5.3 [59].

$$\dot{\phi} = P + \tan\theta\,(Q\sin\phi + R\cos\phi) \tag{5.1}$$

$$\dot{\theta} = Q\cos\phi - R\sin\phi \tag{5.2}$$

$$\dot{\psi} = \frac{Q\sin\phi + R\cos\phi}{\cos\theta} \tag{5.3}$$

In equations 5.1–5.3, P, Q and R are the roll, pitch and yaw rates measured by the gyroscopes and $\dot{\theta}$, $\dot{\phi}$, and $\dot{\psi}$ are the time derivatives of the Euler angles θ, ϕ, and ψ. The Euler angles were assumed to have a value of zero at the beginning of each flight and equations 5.1–5.3 were numerically integrated to calculate the Euler angles of the quadrotor during flight.

Figure 5.12 shows the roll angle (ϕ) recorded during the quadrotor flight. This

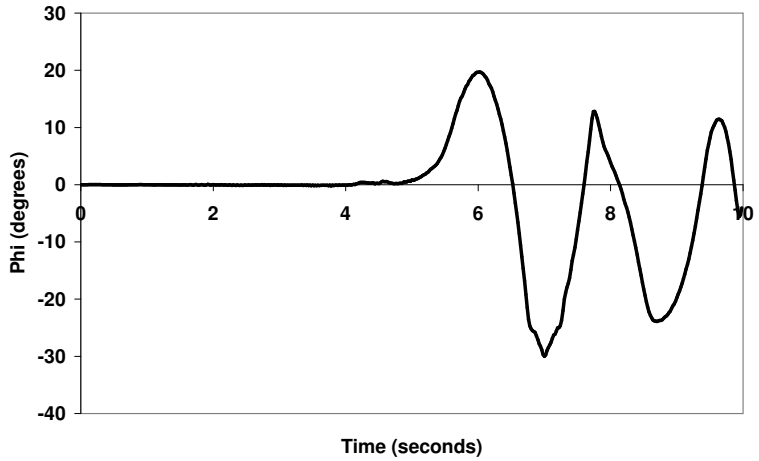

Figure 5.12. A graph of the roll angle phi (ϕ) of the quadrotor during a flight.

graph shows the oscillations in the roll angle that occurred during this flight. The first two peaks were equal to 20 degrees and -30 degrees and then the remaining peaks decreased in magnitude.

Figure 5.13 shows the pitch angle (θ) recorded during the quadrotor flight. Similar to the result for the roll angle, there were large peaks in the pitch angle at the beginning of the flight and the peaks in the pitch angle at the end of the flight

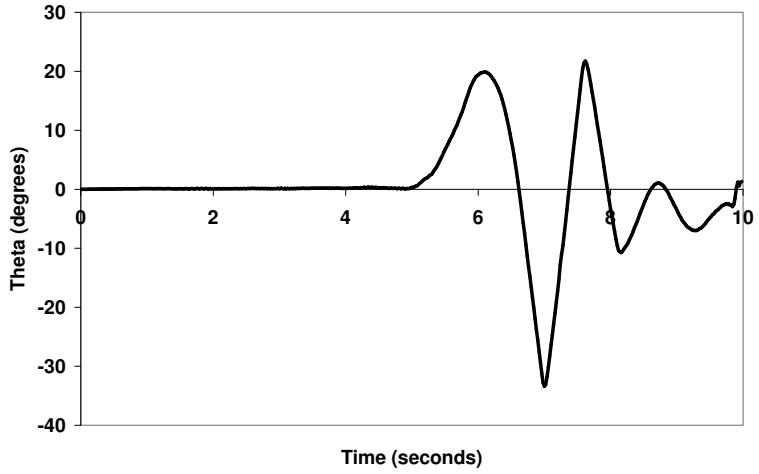

Figure 5.13. A graph of the pitch angle theta (θ) of the quadrotor during a flight.

were smaller in magnitude.

Figure 5.14 shows the yaw angle (ψ) recorded during this flight. The yaw angle was very small until seven seconds into the test when it increased from about zero degrees to roughly -150 degrees. This increase in the yaw angle occurred during the oscillations of the quadrotor over a stationary point. The graphs of the Euler angles in figures 5.12–5.14 match well with the behavior of the quadrotor observed during this flight.

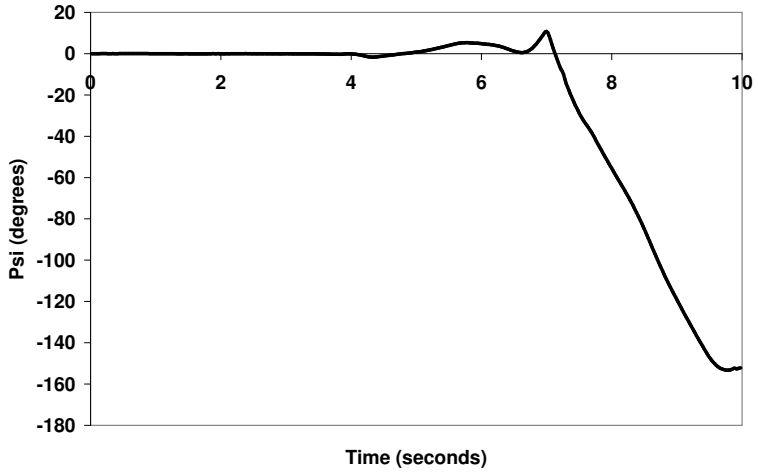

Figure 5.14. A graph of the yaw angle psi (ψ) of the quadrotor during a flight.

Chapter 6

Conclusions

A lightweight quadrotor system has been designed with an emphasis on using inexpensive commercially available components. These components have been integrated with a custom-designed circuit board and software has been developed to interface these components with a microcontroller. A single degree of freedom test system was built to test the integration of these components and a pilot-in-the-loop control law was successfully implemented on this system. The quadrotor was constructed with the electronics needed to develop a stability augmentation system for the quadrotor for about $760. A stability augmentation system was successfully developed for the pitch, roll, and yaw axes of the quadrotor. The quadrotor has been successfully flown by an inexperienced R/C pilot, demonstrating that low-cost components can be used to create a control system that allows manual flight of a quadrotor.

The quadrotor that has been developed for this research can be used in several future research projects. The hardware and software used for this quadrotor can easily be integrated with additional sensors such as cameras, sonar and optic flow

sensors that will allow the level of quadrotor autonomy to be increased. An increase in autonomy will allow operators to be able to learn how to fly the quadrotor very quickly and could allow the operator to perform other tasks while simultaneously flying the quadrotor. A semi-autonomous or autonomous quadrotor has the potential to fly in very confined spaces, such as urban environments or even indoors, with minimal operator interaction. Sensors such as cameras or biological and chemical detectors could also be added to the quadrotor and allow meaningful missions to be performed by this UAV. In addition to the integration of more sensors, future projects can also implement more advanced control schemes, including sensor data fusion and state estimation methods, on the quadrotor. Control algorithms that can overcome any performance shortcomings of the sensors or that can adapt to sensor failures could be especially useful. The current quadrotor could also provide a testbed for research in cooperative control of UAVs or in cooperative efforts between UAVs and unmanned ground vehicles.

Bibliography

[1] Office of the Secretary of Defense. Unmanned Aircraft Systems Roadmap: 2005–2030, 2005.

[2] Laurence R. Newcome. *Unmanned Aviation: A Brief History of Unmanned Aerial Vehicles*. AIAA, 2004.

[3] John D. Anderson, Jr. *Introduction to Flight*. McGraw-Hill Companies, Inc., 5th edition, 2005.

[4] Paul G. Fahlstrom and Thomas J. Gleason. *Introduction to UAV Systems*. Paul G. Fahlstrom and Thomas J. Gleason, 2nd edition, 1998.

[5] Robert C. Michelson and Laurence R. Newcome. AIAA short course in 21st Century Aerial Robotics.

[6] Roger W. Gallington, Harry Berman, John Entzminger, Michael S. Francis, Patrick Palmore, and Jay Stratakes. *Future Aeronautical and Space Systems*, chapter 6. AIAA, 1997. Unmanned Aerial Vehicles.

[7] S. Tsach, J. Chemla, and D. Penn. UAV Systems Development in IAI-Past, Present & Future. In *2nd AIAA "Unmanned Unlimited" Systems, Technologies, and Operations-Aerospace, Land, and Sea Conference*, 2003.

[8] Office of the Secretary of Defense. Unmanned Aerial Vehicles Roadmap: 2002–2027, December 2002.

[9] http://www.noaanews.noaa.gov/stories2005/s2508.htm. October 24, 2005.

[10] Phillip McKerrow. Modelling the Draganflyer four-rotor helicopter. In *Proceedings of the 2004 IEEE International Conference on Robotics and Automation*, 2004.

[11] Huai-yu Wu, Zhao-ying Zhou, and Dong Sun. Autonomous Hovering Control and Test for Micro Air Vehicle. In *Proceedings of the 2003 IEEE International Conference on Robotics and Automation*, 2003.

[12] http://www.yamaha-motor.co.jp/global/business/sky/index.html. November 28, 2005.

[13] http://www.honeywell.com. November 18, 2005.

[14] William J. Pisano, Dale A. Lawrence, and Scott E. Palo. Low-Cost UAV Avionics for Autonomous Antenna Calibration. In *AIAA Infotech@Aerospace Conference*, 2005.

[15] Eric N. Johnson, Daniel P. Schrage, and J.V.R. Prasad. Flight Test Results of Fault Tolerant Control Systems on Small and Micro Rotorcraft. In *AHS International Specialists Meeting on Unmanned Rotorcraft*, 2005.

[16] Joseph K. Conroy, Paul D. Samuel, and Darryll J. Pines. Development of an MAV Control and Navigation System. In *AIAA Infotech@Aerospace Conference*, 2005.

[17] Joseph Conroy, Paul Samuel, and Darryll Pines. The Evaluation of Optic Flow Data using a Wireless Telemetry System for Micro Air Vehicle Applications. In *AHS International Specialists Meeting on Unmanned Rotorcraft*, 2005.

[18] R.M. Barrett. Adaptive Aerostructures: Improving High Performance Subscale Military UAVs. In *45th AIAA/ASME/ASCE/AHS/ASC Structures, Structural Dynamics and Materials Conference*, 2004.

[19] Ron Barrett, Roelof Vos, Paolo Tiso, and Roeland De Breuker. Post-Buckled Precompressed (PBP) Actuators: Enhancing VTOL Autonomous High Speed MAVs. In *46th AIAA/ASME/ASCE/AHS/ASC Structures, Structural Dynamics and Materials Conference*, 2005.

[20] E. Altug, J. P. Ostrowski, and R. Mahony. Control of a Quadrotor Helicopter Using Visual Feedback. In *Proceedings of the IEEE International Conference on Robotics and Automation*, pages 72–7, 2002.

[21] Paul Pounds, Robert Mahony, Joel Gresham, Peter Corke, and Jonathan Roberts. Towards Dynamically-Favourable Quad-Rotor Aerial Robots. In *Proceedings of the 2004 Australasian Conference on Robotics and Automation*, 2004.

[22] P. Pounds, R. Mahony, P. Hynes, and J. Roberts. Design of a Four-Rotor Aerial Robot. In *Proceedings of the 2002 Australasian Conference on Robotics and Automation*, 2002.

[23] J. Gordon Leishman. The Bréguet-Richet Quadrotor Helicopter of 1907. *Vertiflite*, 47(3):58–60, 2002.

[24] Z. Mohammad Zain, N. Mohamad, and Z. Mohamad Ali. Redesign of de Bothezat Helicopter : The Way Forward For the Rotorcraft Industry. In *43rd AIAA/ASME/ASCE/AHS/ASC Structures, Structural Dynamics, and Materials Conference*, 2002.

[25] http://www.cradleofaviation.org/exhibits/jet/quadrotor. August 9, 2005.

[26] http://avia.russian.ee/vertigo/convertawings-r.html. August 9, 2005.

[27] Tarek Hamel, Robert Mahony, Rogelio Lozano, and James Ostrowski. Dynamic Modelling and Configuration Stabilization for an X4-Flyer. In *IFAC 15th Triennial World Congress*, 2002.

[28] Tarek Hamel, Robert Mahony, and Abdelhamid Chriette. Visual servo trajectory tracking for a four rotor VTOL aerial vehicle. In *Proceedings of the IEEE International Conference on Robotics and Automation*, 2002.

[29] Marcus Åberg. 4xFanSaucer. Master's thesis, KTH Signals Sensors and Systems, Stockholm, Sweden, 2004.

[30] Ming Chen and Mihai Huzmezan. A combined MBPC/2 DOF H_∞ controller for a Quad Rotor UAV. In *AIAA Atmospheric Flight Mechanics Conference and Exhibit*, 2003.

[31] http://www.rctoys.com/draganflyer5.php. November 14, 2005.

[32] Richard K. Arning and Stefan Sassen. Flight Control of Micro Aerial Vehicles. In *AIAA Guidance, Navigation, and Control Conference and Exhibit*, 2004.

[33] Jonathan M. Roberts, Peter I. Corke, and Gregg Buskey. Low-Cost Flight Control System for a Small Autonomous Helicopter. In *Proceedings of the 2002 Australasian Conference on Robotics and Automation*, 2002.

[34] E. Altug, J. P. Ostrowski, and C. J. Taylor. Quadrotor Control Using Dual Camera Visual Feedback. In *Proceedings of the IEEE International Conference on Robotics and Automation*, pages 4294–9, 2003.

[35] Matthew G. Earl and Raffaello D'Andrea. Real-Time Attitude Estimation Techniques Applied to a Four Rotor Helicopter. In *Proceeding of the 43rd IEEE Conference on Decision and Control*, 2004.

[36] E. B. Nice. Design of a Four Rotor Hovering Vehicle. Master's thesis, Cornell University, 2004.

[37] http://www.systron.com. November 14, 2005.

[38] Samir Bouabdallah, Andŕe Noth, and Roland Siegwan. PID vs. LQ Control Techniques Applied to an Indoor Micro Quadrotor. In *Proceedings of 2004 IEEE/RSJ International Conference On Intelligent Robots and Systems*, 2004.

[39] http://www.xsens.com. November 14, 2005.

[40] P. Castillo, A. Dzul, and R. Lozano. Real-Time Stabilization and Tracking of a Four-Rotor Mini Rotorcraft. In *IEEE Transactions on Control Systems Technology*, volume 12, pages 510–6, July 2004.

[41] http://www.polhemus.com/fastrak.htm. November 14, 2005.

[42] Gabe Hoffmann, Dev Gorur Rajnarayan, Steven L. Waslander, David Dostal, Jung Soon Jang, and Claire J. Tomlin. The Stanford Testbed of Autonomous Rotorcraft for Multi Agent Control (STARMAC). In *Proceedings of the 23rd Digital Avionics Systems Conference*, 2004.

[43] *PIC18F8720 Data Sheet*, 2004.

[44] Paul Horowitz and Winfield Hill. *The Art of Electronics*. Cambridge University Press, 2nd edition, 1989.

[45] http://www.ccsinfo.com. July 1, 2005.

[46] *Angular Rate Sensor ADXRS150 Data Sheet*, 2004.

[47] *ADXL210E: Low-Cost Dual-Axis Accelerometer with Duty Cycle Data Sheet*, 2004.

[48] *Mini SSC^{TM} II Serial Servo Controller User's Manual*, July 2000.

[49] http://www.futaba-rc.com/radios/index.html. July 11, 2005.

[50] http://www.seetron.com/ssc.htm. July 11, 2005.

[51] *Astro Flight Inc. Aircraft Speed Control Model 217D Data Sheet*.

[52] http://www.motocalc.com. July 11, 2005.

[53] http://www.mpjet.com. August 9, 2005.

[54] http://www.eagletreesystems.com. July 11, 2005.

[55] http://www.cadsoft.de. July 11, 2005.

[56] http://4pcb.com. May 20, 2005.

[57] http://www.robotmarketplace.com. May 20, 2005.

[58] J. Lowen Shearer, Bohdan T. Kulakowski, and John F. Gardner. *Dynamic Modeling and Control of Engineering Systems*. Prentice-Hall, 2nd edition, 1997.

[59] Brian L. Stevens and Frank L. Lewis. *Aircraft Control and Simulation*. John Wiley and Sons, Inc., 2nd edition, 2003.